*Electronic Research Archive*

https://www.aimspress.com/journal/era

ERA, 34(4): 2279–2302.
DOI: 10.3934/era.2026103
Received: 27 January 2026
Revised: 22 February 2026
Accepted: 06 March 2026
Published: 16 March 2026

*Research article*

# Time-delayed dynamics modeling of brucellosis transmission in sheep: precision control strategies driven by age-sex heterogeneity and target reproduction number

**Jun Yang**[1,2], **Boqiang Cao**[1,2] , **Ting Kang**[1,2*] **and Qingyun Wang**[1,2,3]

[1] School of Mathematics and Statistics, Ningxia University, Yinchuan 750021, China

[2] Ningxia Basic Science Research Center of Mathematics, Yinchuan 750021, China

[3] Department of Dynamics and Control, Beihang University, Beijing 100191, China

* **Correspondence:** Email: nxukangting@163.com.

**Abstract:** Brucellosis is a zoonotic disease caused by bacteria of the genus Brucella, posing a significant threats to human health and the development of the livestock industry. Experimental studies have demonstrated significant differences in infection rates among sheep of different ages and sexes. Based on this, this paper develops a time-delayed dynamical model for brucellosis transmission with age-sex structure, coupling the sheep population with environmental contamination, and incorporates a latency time delay to characterize the temporal delay in disease transmission. First, the basic reproduction number is calculated, and the global stability of both disease-free and endemic equilibria is established. Second, for three control measures (i.e., vaccination, isolation of infected sheep, and environmental disinfection) the target reproduction numbers are computed to quantitatively evaluate the relative effectiveness of each strategy in mitigating brucellosis transmission. Numerical simulations reveal that increasing the time delay reduces the number of infected sheep and the concentration of Brucella in the environment. When the target reproduction number exceeds 1, vaccination achieves optimal control efficacy, with required coverage decreasing as the time delay increases. In addition, by adjusting the input rates of female and male lambs and the time delay, the cost-effectiveness of age-based and sex-based vaccination strategies is compared, identifying the parameter regions where each strategy is economically dominant.

**Keywords:** time-delayed dynamical model of brucellosis; target reproduction number; stability; control measures; cost-effectiveness

## 1. Introduction

Brucellosis, also referred to as Mediterranean fever or Malta fever, is a zoonotic infectious disease caused by bacteria of the genus Brucella, posing severe threats to livestock development and public health security. Infected animals (e.g., sheep, cattle, and pigs) and their products serve as the primary sources of infection [1], with transmission occurring through direct contact with infected animals or exposure to contaminated environments [2, 3]. The disease frequently causes infertility and abortion in livestock, and may lead to serious complications in humans, including encephalitis, myelitis, spondylitis, and prostatitis [4]. It is worth noting that brucellosis mainly spreads among animals or from animals to humans, with human-to-human transmission being extremely rare [5]. Therefore, blocking the transmission chain among animals is the core of disease prevention and control.

A substantial body of evidence suggests that brucellosis transmission in sheep is markedly structured by both age and sex: the infection rate of lambs is significantly lower than that of adult sheep, and the infection rate of rams is significantly lower than that of ewes [6, 7]. Based on this epidemiological evidence, scholars have successively constructed dynamical models that take into account age or sex heterogeneity in order to reveal the transmission mechanism of brucellosis and formulate prevention and control strategies [8–10]. For example, Bai et al. [3] constructed a two-stage sheep-environment coupled dynamical model for brucellosis transmission, systematically analyzed the stability of the model's equilibria, and compared the intervention effects of different control measures, providing theoretical support and practical references for the precise prevention and control of brucellosis in sheep. Building upon this foundation, Bai et al. [11] further considered the impact of cross-regional livestock transportation on disease transmission, established a two-patch two-stage model for the transmission dynamics of brucellosis in sheep, and explored the stability of its equilibria; at the same time, based on lamb recruitment rates and basic reproduction numbers in the two patches, they proposed the optimal transportation plans for lambs and adult sheep, providing feasible guidance for blocking the cross-regional transmission of brucellosis. Yang et al. [7] constructed a class of sheep-environment coupled transmission dynamical model with age-sex structure; analyzed the stability of the model's equilibria; and quantitatively evaluated the control effects of vaccination, environmental disinfection, and isolation measures based on the target reproduction number. In addition, they formulated differentiated vaccination strategies according to the input rates of lambs and the costs of vaccination. Meanwhile, time delay, as a key factor influencing the spread of brucellosis, has received extensive attention in epidemic modeling [12–14]. For instance, Hou et al. [15] developed a time delayed susceptible-exposed-infected-Brucella (SEIB) dynamical model with indirect transmission, demonstrating that time delay does not affect the stability of equilibria but can delay the emergence of the infection peak. Lolika et al. [16] analyzed a brucellosis model incorporating two discrete time delays, revealing that delays may induce Hopf bifurcation and consequently lead to periodic solutions. Wu et al. [17] integrated stage structure, seasonality, density-dependent growth, maturation delay, and time-varying latent period to construct a dynamical model of brucellosis transmission. Their research indicates that ignoring time delays can lead to overestimation or underestimation of brucellosis transmission: when the latent period is a constant delay or absent, the number of infected animals will either be higher or lower than that with a periodic delay. However, there are still significant gaps in the above studies: although scholars have explored the effects of age structure or sex heterogeneity [7, 18] on transmission dynamics, no study has yet incorporated the time delay effect and the dual structure of age and sex simultaneously

into the model of sheep brucellosis. This gives rise to three key scientific questions: (1) How can a transmission dynamical model be constructed that explicitly characterizes the coupling of age-sex stratification and time delay? (2) How can the effectiveness of prevention and control measures, such as vaccination, environmental disinfection, and isolation of infected sheep, be quantitatively evaluated? What regulatory roles does time delay play in these measures? (3) Which specific groups (e.g., lambs, adult sheep, ewes, or rams) should be targeted for intervention to achieve optimal cost-effectiveness?

To address the above questions systematically, the remainder of this paper is organized as follows: Section 2 establishes a sheep-environment coupled time delayed dynamical model for brucellosis transmission, incorporating age and sex heterogeneous infectivity. The existence and stability of the model's equilibria are analyzed in Sections 3 and 4, respectively. Section 5 introduces the target reproduction number in the time-delayed context and derives its expressions for three control measures: vaccination, environmental disinfection, and isolation of infected sheep. Section 6 validates the theoretical results through numerical simulations, evaluates the effectiveness of the three control measures, and further investigates how time delay modulates brucellosis transmission and control efficacy. Finally, Section 7 summarizes the main findings and outlines promising directions for future research.

## 2. Dynamical model

The infection characteristics and transmission mechanisms of brucellosis exhibit significant population heterogeneity and environmental dependence. At the host level, the infection rate varies differently by gender and age. In terms of sex, the infection rate of ewes is significantly higher than that of rams, where adult or sexually mature ewes have an especially high risk of infection due to increased exposure to pathogens through physiological activities, such as pregnancy and childbirth [7, 18]. In terms of age, adult sheep are more susceptible than lambs [10, 19]. At the environmental level, infected sheep acts as the main source of infection, releasing Brucella into the environment through aborted fetuses, placentas, and excretions. Brucella exhibits extremely strong survival capabilities outside the body, surviving for weeks in feces at room temperature and even months under favorable conditions. This characteristic significantly increases the risk of indirect transmission [20, 21]. Based on these epidemiological features, the following simplifications are made in model formulation:

(i) Regarding the age-sex structure, since the environmental-host transmission efficiency is relatively low and there is a significant difference in susceptibility between lambs and adult sheep [10, 19], the indirect transmission only distinguishes between the two age groups of lambs and adult sheep, and sex differences are not considered for the time being.

(ii) Based on references [2, 10], it is known that infected sheep during the incubation period are undetectable, and the infectivity during this period remains unclear. Furthermore, reference [22] indicates that the infectivity of infected animals in the early stage of incubation is almost zero, and hosts only excrete Brucella and exhibit a certain degree of infectivity in the late stage of incubation. Therefore, we disregard the infectivity of sheep during the incubation period.

Based on the above considerations, the sheep population $N(t)$ is divided into six categories (i.e., $S_{11}(t)$, $S_{12}(t)$, $S_{21}(t)$, $S_{22}(t)$, $E(t)$, and $I(t)$), which represent the number of susceptible ram lambs, rams, ewe lambs, ewes, exposed sheep, and infected sheep at time $t$, respectively. $W(t)$ denotes the

Brucella load in the environment at time $t$. The total sheep population at time $t$ can be expressed as

$$N(t) = S_{11}(t) + S_{12}(t) + S_{21}(t) + S_{22}(t) + E(t) + I(t).$$

For simplicity, we abbreviate $S_{11}(t), S_{12}(t), S_{21}(t), S_{22}(t), E(t), I(t), W(t)$, and $N(t)$ as $S_{11}, S_{12}, S_{21}$, $S_{22}, E, I, W$, and $N$, respectively. $\tau \geq 0$ denotes the time delay characterizing the latent period of brucellosis and the transition rate from exposed sheep to infected sheep at time $t$ is given by $[\beta_{11}S_{11}(t-\tau)+\beta_{12}S_{12}(t-\tau)+\beta_{21}S_{21}(t-\tau)+\beta_{22}S_{22}(t-\tau)]I(t-\tau)e^{-\mu_3\tau} + [\varphi_1 S_{11}(t-\tau)+\varphi_2 S_{12}(t-\tau)+\varphi_1 S_{21}(t-\tau)+\varphi_2 S_{22}(t-\tau)]W(t-\tau)e^{-\mu_3\tau}$. Thus, the transmission flowchart of brucellosis among sheep of different ages and sexes is shown in Figure 1, and the dynamical model is formulated as follows:

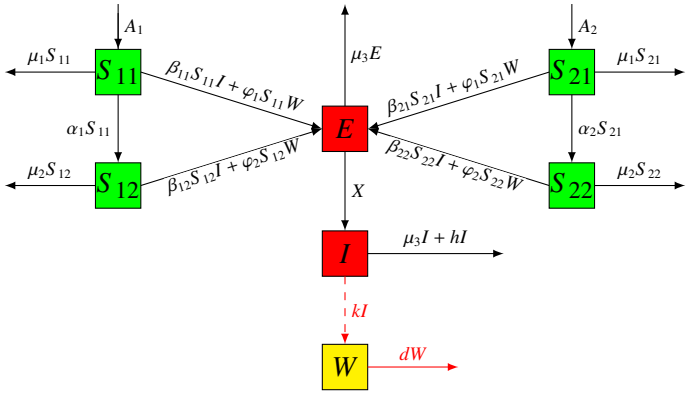


**Figure 1.** Transmission flowchart of sheep brucellosis (the black arrows indicate the transferring of sheep, while the red arrows represent the transferring of Brucella and $X = [\beta_{11}S_{11}(t-\tau)+\beta_{12}S_{12}(t-\tau)+\beta_{21}S_{21}(t-\tau)+\beta_{22}S_{22}(t-\tau)]I(t-\tau)e^{-\mu_3\tau} + [\varphi_1 S_{11}(t-\tau)+\varphi_2 S_{12}(t-\tau)+\varphi_1 S_{21}(t-\tau)+\varphi_2 S_{22}(t-\tau)]W(t-\tau)e^{-\mu_3\tau}$).

$$\begin{cases}
\dfrac{dS_{11}}{dt} = A_1 - \beta_{11}S_{11}I - \varphi_1 S_{11}W - \alpha_1 S_{11} - \mu_1 S_{11}, \\
\dfrac{dS_{12}}{dt} = \alpha_1 S_{11} - \beta_{12}S_{12}I - \varphi_2 S_{12}W - \mu_2 S_{12}, \\
\dfrac{dS_{21}}{dt} = A_2 - \beta_{21}S_{21}I - \varphi_1 S_{21}W - \alpha_2 S_{21} - \mu_1 S_{21}, \\
\dfrac{dS_{22}}{dt} = \alpha_2 S_{21} - \beta_{22}S_{22}I - \varphi_2 S_{22}W - \mu_2 S_{22}, \\
\dfrac{dE}{dt} = (\beta_{11}S_{11} + \beta_{12}S_{12} + \beta_{21}S_{21} + \beta_{22}S_{22})I + (\varphi_1 S_{11} + \varphi_2 S_{12} + \varphi_1 S_{21} + \varphi_2 S_{22})W \\
\qquad - [\beta_{11}S_{11}(t-\tau) + \beta_{12}S_{12}(t-\tau) + \beta_{21}S_{21}(t-\tau) + \beta_{22}S_{22}(t-\tau)]I(t-\tau)e^{-\mu_3\tau} \\
\qquad - [\varphi_1 S_{11}(t-\tau) + \varphi_2 S_{12}(t-\tau) + \varphi_1 S_{21}(t-\tau) + \varphi_2 S_{22}(t-\tau)]W(t-\tau)e^{-\mu_3\tau} - \mu_3 E, \\
\dfrac{dI}{dt} = [\beta_{11}S_{11}(t-\tau) + \beta_{12}S_{12}(t-\tau) + \beta_{21}S_{21}(t-\tau) + \beta_{22}S_{22}(t-\tau)]I(t-\tau)e^{-\mu_3\tau} \\
\qquad + [\varphi_1 S_{11}(t-\tau) + \varphi_2 S_{12}(t-\tau) + \varphi_1 S_{21}(t-\tau) + \varphi_2 S_{22}(t-\tau)]W(t-\tau)e^{-\mu_3\tau} \\
\qquad - \mu_3 I - hI, \\
\dfrac{dW}{dt} = kI - dW.
\end{cases} \tag{2.1}$$

All parameters in model (2.1) are non-negative and the biological meanings are shown in Table 1. The initial conditions for model (2.1) take the following form:

$$S_{11}(\theta) = \phi_1(\theta), S_{12}(\theta) = \phi_2(\theta), S_{21}(\theta) = \phi_3(\theta), S_{22}(\theta) = \phi_4(\theta), E(\theta) = \phi_5(\theta),$$
$$I(\theta) = \phi_6(\theta), W(\theta) = \phi_7(\theta), \theta \in [-\tau, 0],$$

where $\phi_i(\theta)(i = 1, 2, \cdots, 7)$ is a continuous function with domain $[-\tau, 0]$ and range in $R^+$ and the sup-norm is $\|\phi\| = \sup_{x\in[-\tau,0]} |\phi(x)|$.

**Table 1.** The biological meanings of the model parameters.

| Parameter | Meanings |
|---|---|
| $A_1$ | Input rate of the ram lambs |
| $A_2$ | Input rate of the ewe lambs |
| $\beta_{11}$ | Transmission rate between infected sheep and ram lambs |
| $\beta_{12}$ | Transmission rate between infected sheep and rams |
| $\beta_{21}$ | Transmission rate between infected sheep and ewe lambs |
| $\beta_{22}$ | Transmission rate between infected sheep and ewes |
| $\varphi_1$ | Transmission rate from Brucella to susceptible lambs |
| $\varphi_2$ | Transmission rate from Brucella to susceptible adult sheep |
| $\mu_1$ | Natural mortality rate of lambs |
| $\mu_2$ | Natural mortality rate of adult sheep |
| $\mu_3$ | Natural mortality of exposed and infected sheep ($\mu_1 \le \mu_3 \le \mu_2$) |
| $h$ | Slaughter rate of infected sheep |
| $k$ | Emission rate of Brucella from infected sheep to the environment |
| $d$ | Apoptosis rate of Brucella in the environment |
| $\alpha_1$ | Transition rate from ram lambs to rams |
| $\alpha_2$ | Transition rate from ewe lambs to ewes |

For continuity of the initial conditions, we need to further require

$$E(0) = \int_{-\tau}^{0} \sum_{i,j=1}^{2} \beta_{ij} S_{ij}(\theta) I(\theta) e^{\mu_3 \theta} d\theta + \int_{-\tau}^{0} \sum_{i=1}^{2} \varphi_1 S_{i1}(\theta) W(\theta) e^{\mu_3 \theta} d\theta$$
$$+ \int_{-\tau}^{0} \sum_{i=1}^{2} \varphi_2 S_{i2}(\theta) W(\theta) e^{\mu_3 \theta} d\theta.$$

Furthermore, through simple calculations, we derive that the positively invariant set of system (2.1) is

$$\Gamma = \left\{ (S_{11}, S_{12}, S_{21}, S_{22}, E, I, W) \in \mathbb{R}^7_+ : \| \sum_{i,j=1}^{2} S_{ij} + E + I \| \le \frac{A_1 + A_2}{\mu}, \|W\| \le \frac{k(A_1 + A_2)}{d\mu} \right\},$$

where $\mathbb{R}^7_+ = \{(x_1, x_2, \cdots, x_7) | x_i \ge 0, i = 1, 2, \cdots, 7\}$, $\mu = \min\{\mu_1, \mu_2, \mu_3\}$.

## 3. Existence of equilibria and basic reproduction number

### 3.1. Disease-free equilibrium and basic reproduction number

The disease-free equilibrium of model (2.1) is

$$P^0 = \left(\frac{A_1}{\mu_1+\alpha_1}, \frac{\alpha_1 A_1}{\mu_2(\mu_1+\alpha_1)}, \frac{A_2}{\mu_1+\alpha_2}, \frac{\alpha_2 A_2}{\mu_2(\mu_1+\alpha_2)}, 0, 0, 0\right).$$

Denoting $f_1 = \beta_{11}S_{11}^0 + \beta_{12}S_{12}^0 + \beta_{21}S_{21}^0 + \beta_{22}S_{22}^0$ and $f_2 = \varphi_1 S_{11}^0 + \varphi_2 S_{12}^0 + \varphi_1 S_{21}^0 + \varphi_2 S_{22}^0$ and using the next generation matrix method [23, 24], we can derive the basic reproduction number

$$\begin{aligned}\mathscr{R}_0 &= \frac{f_1}{\mu_3+h}e^{-\mu_3\tau} + \frac{kf_2}{d(\mu_3+h)}e^{-\mu_3\tau}\\ &\triangleq \mathscr{R}_{01} + \mathscr{R}_{02},\end{aligned}$$

where $\mathscr{R}_{01}$ and $\mathscr{R}_{02}$ denote the expected number of secondary infections generated by direct transmission from one infected sheep and by indirect transmission via environmental contamination per unit time, respectively.

### 3.2. Existence and uniqueness of endemic equilibrium

In this subsection, we will prove the existence and uniqueness of the endemic equilibrium.

**Theorem 3.1.** *There exists a unique endemic equilibrium $P^*$ of model (2.1) when $\mathscr{R}_0 > 1$.*

*Proof.* We prove this theorem by the following two steps:

**Step 1: Existence**. The endemic equilibrium $P^* = (S_{11}^*, S_{12}^*, S_{21}^*, S_{22}^*, E^*, I^*, W^*)$ satisfies

$$\begin{cases} A_1 - \beta_{11}S_{11}^*I^* - \varphi_1 S_{11}^*W^* - \alpha_1 S_{11}^* - \mu_1 S_{11}^* = 0,\\ \alpha_1 S_{11}^* - \beta_{12}S_{12}^*I^* - \varphi_2 S_{12}^*W^* - \mu_2 S_{12}^* = 0,\\ A_2 - \beta_{21}S_{21}^*I^* - \varphi_1 S_{21}^*W^* - \alpha_2 S_{21}^* - \mu_1 S_{21}^* = 0,\\ \alpha_2 S_{21}^* - \beta_{22}S_{22}^*I^* - \varphi_2 S_{22}^*W^* - \mu_2 S_{22}^* = 0,\\ (\beta_{11}S_{11}^* + \beta_{12}S_{12}^* + \beta_{21}S_{21}^* + \beta_{22}S_{22}^*)I^* + (\varphi_1 S_{11}^* + \varphi_2 S_{12}^* + \varphi_1 S_{21}^*\\ \quad +\varphi_2 S_{22}^*)W^* - (\beta_{11}S_{11}^* + \beta_{12}S_{12}^* + \beta_{21}S_{21}^* + \beta_{22}S_{22}^*)I^*e^{-\mu_3\tau}\\ \quad -(\varphi_1 S_{11}^* + \varphi_2 S_{12}^* + \varphi_1 S_{21}^* + \varphi_2 S_{22}^*)W^*e^{-\mu_3\tau} - \mu_3 E^* = 0,\\ [(\beta_{11}S_{11}^* + \beta_{12}S_{12}^* + \beta_{21}S_{21}^* + \beta_{22}S_{22}^*)I^* + (\varphi_1 S_{11}^* + \varphi_2 S_{12}^*\\ \quad +\varphi_1 S_{21}^* + \varphi_2 S_{22}^*)W^*]e^{-\mu_3\tau} - \mu_3 I^* - hI^* = 0,\\ kI^* - dW^* = 0. \end{cases} \tag{3.1}$$

By calculating, we can obtain

$$\begin{aligned} W^* &= \frac{k}{d}I^*,\\ S_{11}^* &= \frac{dA_1}{d\beta_{11}I^* + \varphi_1 kI^* + d\alpha_1 + d\mu_1}, \end{aligned}$$

$$
\begin{aligned}
S_{12}^* =& \frac{d\alpha_1}{d\beta_{12}I^* + \varphi_2 kI^* + d\mu_2} \cdot \frac{dA_1}{d\beta_{11}I^* + \varphi_1 kI^* + d\alpha_1 + d\mu_1},\\
S_{21}^* =& \frac{dA_2}{d\beta_{21}I^* + \varphi_1 kI^* + d\alpha_2 + d\mu_1},\\
S_{22}^* =& \frac{d\alpha_2}{d\beta_{22}I^* + \varphi_2 kI^* + d\mu_2} \cdot \frac{dA_2}{d\beta_{21}I^* + \varphi_1 kI^* + d\alpha_2 + d\mu_1},\\
E^* =& \frac{1}{\mu_3}\Big[(\beta_{11}S_{11}^* + \beta_{12}S_{12}^* + \beta_{21}S_{21}^* + \beta_{22}S_{22}^*)I^* + (\varphi_1 S_{11}^* + \varphi_2 S_{12}^*\\
&+ \varphi_1 S_{21}^* + \varphi_2 S_{22}^*)W^* - (\beta_{11}S_{11}^* + \beta_{12}S_{12}^* + \beta_{21}S_{21}^* + \beta_{22}S_{22}^*)I^* e^{-\mu_3\tau}\\
&- (\varphi_1 S_{11}^* + \varphi_2 S_{12}^* + \varphi_1 S_{21}^* + \varphi_2 S_{22}^*)W^* e^{-\mu_3\tau}\Big].
\end{aligned}
$$

Substituting $S_{11}^*, S_{12}^*, S_{21}^*, S_{22}^*, E^*$, and $W^*$ into the sixth equation of (3.1), we have

$$
\begin{aligned}
&e^{-\mu_3\tau}\Big[\frac{A_1(d\beta_{11} + \varphi_1 k)}{d\beta_{11}I^* + \varphi_1 kI^* + d\alpha_1 + d\mu_1} + \frac{A_2(d\beta_{21} + \varphi_1 k)}{d\beta_{21}I^* + \varphi_1 kI^* + d\alpha_2 + d\mu_1} + \frac{dA_1\alpha_1(d\beta_{12} + \varphi_2 k)}{d\beta_{12}I^* + \varphi_2 kI^* + d\mu_2}\\
&\cdot \frac{1}{d\beta_{11}I^* + \varphi_1 kI^* + d\alpha_1 + d\mu_1} + \frac{dA_2\alpha_2(d\beta_{22} + \varphi_2 k)}{d\beta_{22}I^* + \varphi_2 kI^* + d\mu_2} \cdot \frac{1}{d\beta_{21}I^* + \varphi_1 kI^* + d\alpha_2 + d\mu_1}\Big] - \mu_3 - h = 0,
\end{aligned}
$$

Furthermore, we denote the above equation as $F(I^*) = 0$. Obviously,

$$
\begin{aligned}
\lim_{I^*\to 0^+} F(I^*) &= (\mu_3 + h)\Big[\frac{\frac{\beta_{11}A_1}{\alpha_1+\mu_1} + \frac{\beta_{12}\alpha_1 A_1}{\mu_2(\alpha_1+\mu_1)} + \frac{\beta_{21}A_2}{\mu_1+\alpha_2} + \frac{\beta_{22}\alpha_2 A_2}{\mu_2(\mu_1+\alpha_2)}}{\mu_3 + h} e^{-\mu_3\tau}\\
&\quad + \frac{k\left(\frac{\varphi_1 A_1}{\alpha_1+\mu_1} + \frac{\varphi_2\alpha_1 A_1}{\mu_2(\alpha_1+\mu_1)} + \frac{\varphi_1 A_2}{\mu_1+\alpha_2} + \frac{\varphi_2\alpha_2 A_2}{\mu_2(\mu_1+\alpha_2)}\right)}{d(\mu_3 + h)} e^{-\mu_3\tau} - 1\Big]\\
&= (\mu_3 + h)(\mathscr{R}_0 - 1) > 0, \qquad (3.2)\\
\lim_{I^*\to+\infty} F(I^*) &= -\mu_3 - h < 0. \qquad (3.3)
\end{aligned}
$$

According to (3.2) and (3.3), there must be at least one zero point on the interval $(0, +\infty)$. In other words, there must exist at least one endemic equilibrium.

**Step 2: Uniqueness**. Since the derivative of $F(I^*)$ is

$$
\begin{aligned}
F'(I^*) = &-\frac{A_1(d\beta_{11} + \varphi_1 k)^2}{(d\beta_{11}I^* + \varphi_1 kI^* + d\alpha_1 + d\mu_1)^2} e^{-\mu_3\tau} - \frac{dA_1\alpha_1(d\beta_{12} + \varphi_2 k)^2}{(d\beta_{12}I^* + \varphi_2 kI^* + d\mu_2)^2}\\
&\cdot \frac{1}{d\beta_{11}I^* + \varphi_1 kI^* + d\alpha_1 + d\mu_1} e^{-\mu_3\tau} - \frac{dA_1\alpha_1(d\beta_{12} + \varphi_2 k)}{d\beta_{12}I^* + \varphi_2 kI^* + d\mu_2}\\
&\cdot \frac{d\beta_{11} + \varphi_1 k}{(d\beta_{11}I^* + \varphi_1 kI^* + d\alpha_1 + d\mu_1)^2} e^{-\mu_3\tau} - \frac{A_2(d\beta_{21} + \varphi_1 k)^2}{(d\beta_{21}I^* + \varphi_1 kI^* + d\alpha_2 + d\mu_1)^2} e^{-\mu_3\tau}\\
&- \frac{dA_2\alpha_2(d\beta_{22} + \varphi_2 k)^2}{(d\beta_{22}I^* + \varphi_2 kI^* + d\mu_2)^2} \cdot \frac{1}{d\beta_{21}I^* + \varphi_1 kI^* + d\alpha_2 + d\mu_1} e^{-\mu_3\tau}\\
&- \frac{dA_2\alpha_2(d\beta_{22} + \varphi_2 k)}{d\beta_{22}I^* + \varphi_2 kI^* + d\mu_2} \cdot \frac{d\beta_{21} + \varphi_1 k}{(d\beta_{21}I^* + \varphi_1 kI^* + d\alpha_2 + d\mu_1)^2} e^{-\mu_3\tau} < 0,
\end{aligned}
$$

the function $F(I^*)$ is strictly monotonically decreasing on the interval $(0, +\infty)$.

Combining Steps 1 and 2, there exists a unique endemic equilibrium $P^*$ for model (2.1) when $\mathscr{R}_0 > 1$. □

## 4. The stability of equilibria

Model (2.1) can be decoupled into the following model

$$\begin{cases} \dfrac{\mathrm{d}S_{11}}{\mathrm{d}t} = A_1 - \beta_{11}S_{11}I - \varphi_1 S_{11}W - \alpha_1 S_{11} - \mu_1 S_{11}, \\ \dfrac{\mathrm{d}S_{12}}{\mathrm{d}t} = \alpha_1 S_{11} - \beta_{12}S_{12}I - \varphi_2 S_{12}W - \mu_2 S_{12}, \\ \dfrac{\mathrm{d}S_{21}}{\mathrm{d}t} = A_2 - \beta_{21}S_{21}I - \varphi_1 S_{21}W - \alpha_2 S_{21} - \mu_1 S_{21}, \\ \dfrac{\mathrm{d}S_{22}}{\mathrm{d}t} = \alpha_2 S_{21} - \beta_{22}S_{22}I - \varphi_2 S_{22}W - \mu_2 S_{22}, \\ \dfrac{\mathrm{d}I}{\mathrm{d}t} = [\beta_{11}S_{11}(t-\tau) + \beta_{12}S_{12}(t-\tau) + \beta_{21}S_{21}(t-\tau) + \beta_{22}S_{22}(t-\tau)]I(t-\tau)e^{-\mu_3\tau} \\ \qquad\quad + [\varphi_1 S_{11}(t-\tau) + \varphi_2 S_{12}(t-\tau) + \varphi_1 S_{21}(t-\tau) + \varphi_2 S_{22}(t-\tau)]W(t-\tau)e^{-\mu_3\tau} \\ \qquad\quad - \mu_3 I - hI, \\ \dfrac{\mathrm{d}W}{\mathrm{d}t} = kI - dW. \end{cases} \tag{4.1}$$

### 4.1. The stability of the disease-free equilibrium

**Theorem 4.1.** *The disease-free equilibrium $P^0$ is globally asymptotically stable when $\mathscr{R}_0 < 1$.*

*Proof.* Define the Lyapunov function $V_1$ as follows:

$$\begin{aligned} V_1 = {} & S_{11}^0 g\left(\frac{S_{11}}{S_{11}^0}\right) + S_{12}^0 g\left(\frac{S_{12}}{S_{12}^0}\right) + S_{21}^0 g\left(\frac{S_{21}}{S_{21}^0}\right) + S_{22}^0 g\left(\frac{S_{22}}{S_{22}^0}\right) + e^{\mu_3\tau} I \\ & + \frac{\varphi_1 S_{11}^0 + \varphi_2 S_{12}^0 + \varphi_1 S_{21}^0 + \varphi_2 S_{22}^0}{d} W + \beta_{11}\int_{t-\tau}^{t} S_{11}(\theta)I(\theta)d\theta \\ & + \beta_{12}\int_{t-\tau}^{t} S_{12}(\theta)I(\theta)d\theta + \beta_{21}\int_{t-\tau}^{t} S_{21}(\theta)I(\theta)d\theta + \beta_{22}\int_{t-\tau}^{t} S_{22}(\theta)I(\theta)d\theta \\ & + \varphi_1\int_{t-\tau}^{t} S_{11}(\theta)W(\theta)d\theta + \varphi_2\int_{t-\tau}^{t} S_{12}(\theta)W(\theta)d\theta + \varphi_1\int_{t-\tau}^{t} S_{21}(\theta)W(\theta)d\theta \\ & + \varphi_2\int_{t-\tau}^{t} S_{22}(\theta)W(\theta)d\theta, \end{aligned} \tag{4.2}$$

where function $g : (0, +\infty) \to [0, +\infty)$ is defined as $g(x) = x - 1 - \ln x$ and $b_1 = \frac{1}{k}[(\mu_3 + h) - (\beta_{11}S_{11}^0 + \beta_{12}S_{12}^0 + \beta_{21}S_{21}^0 + \beta_{22}S_{22}^0)] > 0$. Calculating the derivative of (4.2) along the solutions of model (4.1), we obtain

$$\frac{\mathrm{d}V_1}{\mathrm{d}t} = \left(1 - \frac{S_{11}^0}{S_{11}}\right)(A_1 - \beta_{11}S_{11}I - \varphi_1 S_{11}W - \alpha_1 S_{11} - \mu_1 S_{11})$$

$$
\begin{aligned}
&+ (1 - \frac{S^0_{12}}{S_{12}})(\alpha_1 S_{11} - \beta_{12} S_{12} I - \varphi_2 S_{12} W - \mu_2 S_{12}) \\
&+ (1 - \frac{S^0_{21}}{S_{21}})(A_2 - \beta_{21} S_{21} I - \varphi_1 S_{21} W - \mu_1 S_{21} - \alpha_2 S_{21}) \\
&+ (1 - \frac{S^0_{22}}{S_{22}})(\alpha_2 S_{21} - \beta_{22} S_{22} I - \varphi_2 S_{22} W - \mu_2 S_{22}) \\
&+ e^{\mu_3 \tau}\{[\beta_{11} S_{11}(t-\tau) + \beta_{12} S_{12}(t-\tau) + \beta_{21} S_{21}(t-\tau) + \beta_{22} S_{22}(t-\tau)] I(t-\tau) e^{-\mu_3 \tau} \\
&+ [\varphi_1 S_{11}(t-\tau) + \varphi_2 S_{12}(t-\tau) + \varphi_1 S_{21}(t-\tau) + \varphi_2 S_{22}(t-\tau)] W(t-\tau) e^{-\mu_3 \tau} \\
&- \mu_3 I - hI\} + \frac{\varphi_1 S^0_{11} + \varphi_2 S^0_{12} + \varphi_1 S^0_{21} + \varphi_2 S^0_{22}}{d}(kI - dW) \\
&+ \beta_{11} S_{11} I - \beta_{11} S_{11}(t-\tau) I(t-\tau) + \beta_{12} S_{12} I - \beta_{12} S_{12}(t-\tau) I(t-\tau) \\
&+ \beta_{21} S_{21} I - \beta_{21} S_{21}(t-\tau) I(t-\tau) + \beta_{22} S_{22} I - \beta_{22} S_{22}(t-\tau) I(t-\tau) \\
&+ \varphi_1 S_{11} W - \varphi_1 S_{11}(t-\tau) W(t-\tau) + \varphi_2 S_{12} W - \varphi_2 S_{12}(t-\tau) W(t-\tau) \\
&+ \varphi_1 S_{21} W - \varphi_1 S_{21}(t-\tau) W(t-\tau) + \varphi_2 S_{22} W - \varphi_2 S_{22}(t-\tau) W(t-\tau) \\
= \; & - A_1 g\Big(\frac{S^0_{11}}{S_{11}}\Big) - \mu_1 S^0_{11} g\Big(\frac{S_{11}}{S^0_{11}}\Big) - \alpha_1 S^0_{11}\Big[g\Big(\frac{S_{12}}{S^0_{12}}\Big) + g\Big(\frac{S^0_{12} S_{11}}{S^0_{11} S_{12}}\Big)\Big] \\
&- A_2 g\Big(\frac{S^0_{21}}{S_{21}}\Big) - \mu_1 S^0_{21} g\Big(\frac{S_{21}}{S^0_{21}}\Big) - \alpha_2 S^0_{21}\Big[g\Big(\frac{S_{22}}{S^0_{22}}\Big) + g\Big(\frac{S_{21} S^0_{22}}{S^0_{21} S_{22}}\Big)\Big] \\
&+ e^{\mu_3 \tau}(\mu_3 + h)(\mathscr{R}_0 - 1) I \\
\le \; & 0.
\end{aligned}
$$

Denote $\mathbb{S} \triangleq \Big\{(S_{11}, S_{12}, S_{21}, S_{22}, I, W) \in \Gamma : \frac{\mathrm{d}V_1}{\mathrm{d}t} = 0\Big\}$. When $\mathscr{R}_0 < 1$, $\frac{\mathrm{d}V_1}{\mathrm{d}t} = 0$ implies $S_{11} = S^0_{11}, S_{12} = S^0_{12}, S_{21} = S^0_{21}, S_{22} = S^0_{22}, I = 0$. Let $(S_{11}(t), S_{12}(t), S_{21}(t), S_{22}(t), I(t), W(t))$ be a solution to model (4.1) that lies in set $\mathbb{S}$ for all time. Then, $I \equiv 0$ implies $\frac{\mathrm{d}I}{\mathrm{d}t} \equiv 0$, which in turn implies $W \equiv 0$. Thus, the only solution to model (4.1) that lies in set $\mathbb{S}$ for all time is the trivial solution $(S_{11}(t), S_{12}(t), S_{21}(t), S_{22}(t), I(t), W(t)) = (S^0_{11}, S^0_{12}, S^0_{21}, S^0_{22}, 0, 0)$. According to LaSalle's invariance principle, the disease-free equilibrium $P^0$ is globally asymptotically stable when $\mathscr{R}_0 < 1$. □

### *4.2. The stability of the endemic equilibrium*

**Theorem 4.2.** *The endemic equilibrium $P^*$ of model (4.1) is globally asymptotically stable if $\mathscr{R}_0 > 1$.*

Define the Lyapunov function $V_2$ as follows:

$$
V_2 = S^*_{11} g\left(\frac{S_{11}}{S^*_{11}}\right) + S^*_{12} g\left(\frac{S_{12}}{S^*_{12}}\right) + S^*_{21} g\left(\frac{S_{21}}{S^*_{21}}\right) + S^*_{22} g\left(\frac{S_{22}}{S^*_{22}}\right) + a_1 I^* g\left(\frac{I}{I^*}\right) + a_2 W^* g\left(\frac{W}{W^*}\right), \tag{4.3}
$$

where $a_1$ and $a_2$ are positive constants to be determined later. Differentiating $V_2$ along the direction of the solutions to the model, we can obtain

$$
\frac{\mathrm{d}V_2}{\mathrm{d}t} = \left(1 - \frac{S^*_{11}}{S_{11}}\right)(A_1 - \beta_{11} S_{11} I - \varphi_1 S_{11} W - \alpha_1 S_{11} - \mu_1 S_{11})
$$

$$
\begin{aligned}
&+\left(1-\frac{S_{12}^*}{S_{12}}\right)(\alpha_1 S_{11}-\beta_{12}S_{12}I-\varphi_2 S_{12}W-\mu_2 S_{12})\\
&+\left(1-\frac{S_{21}^*}{S_{21}}\right)(A_2-\beta_{21}S_{21}I-\varphi_1 S_{21}W-\mu_1 S_{21}-\alpha_2 S_{21})\\
&+\left(1-\frac{S_{22}^*}{S_{22}}\right)(\alpha_2 S_{21}-\beta_{22}S_{22}I-\varphi_2 S_{22}W-\mu_2 S_{22})\\
&+a_1\left(1-\frac{I^*}{I}\right)[(\beta_{11}S_{11}(t-\tau)+\beta_{12}S_{12}(t-\tau)+\beta_{21}S_{21}(t-\tau)+\beta_{22}S_{22}(t-\tau))\\
&\cdot I(t-\tau)e^{-\mu_3\tau}+(\varphi_1 S_{11}(t-\tau)+\varphi_2 S_{12}(t-\tau)+\varphi_1 S_{21}(t-\tau)+\varphi_2 S_{22}(t-\tau))\\
&\cdot W(t-\tau)e^{-\mu_3\tau}-\mu_3 I-hI]+a_2\left(1-\frac{W^*}{W}\right)(kI-dW)\,. \qquad (4.4)
\end{aligned}
$$

For simplicity, we denote

$$
\begin{aligned}
&x_1=\frac{S_{11}}{S_{11}^*},x_2=\frac{S_{12}}{S_{12}^*},x_3=\frac{S_{21}}{S_{21}^*},x_4=\frac{S_{22}}{S_{22}^*},x_{1,\tau}=\frac{S_{11}(t-\tau)}{S_{11}^*},\\
&x_{2,\tau}=\frac{S_{12}(t-\tau)}{S_{12}^*},x_{3,\tau}=\frac{S_{21}(t-\tau)}{S_{21}^*},x_{4,\tau}=\frac{S_{22}(t-\tau)}{S_{22}^*},y=\frac{I}{I^*}\\
&y_\tau=\frac{I(t-\tau)}{I^*},z=\frac{W}{W^*},z_\tau=\frac{W(t-\tau)}{W^*}.
\end{aligned}
$$

Then, (4.4) becomes

$$
\begin{aligned}
\frac{\mathrm{d}V_2}{\mathrm{d}t}&=\left(1-\frac{1}{x_1}\right)(A_1-\beta_{11}x_1S_{11}^*yI^*-\varphi_1x_1S_{11}^*W^*z-\alpha_1x_1S_{11}^*-\mu_1x_1S_{11}^*)\\
&+\left(1-\frac{1}{x_2}\right)(\alpha_1x_1S_{11}^*-\beta_{12}x_2S_{12}^*yI^*-\varphi_2x_2S_{12}^*W^*z-\mu_2x_2S_{12}^*)\\
&+\left(1-\frac{1}{x_3}\right)(A_2-\beta_{21}x_3S_{21}^*yI^*-\varphi_1x_3S_{21}^*W^*z-\mu_1x_3S_{21}^*-\alpha_2x_3S_{21}^*)\\
&+\left(1-\frac{1}{x_4}\right)(\alpha_2x_3S_{21}^*-\beta_{22}x_4S_{22}^*yI^*-\varphi_2x_4S_{22}^*W^*z-\mu_2x_4S_{22}^*)\\
&+a_1\left(1-\frac{1}{y}\right)[(\beta_{11}x_{1,\tau}S_{11}^*+\beta_{12}x_{2,\tau}S_{12}^*+\beta_{21}x_{3,\tau}S_{21}^*+\beta_{22}x_{4,\tau}S_{22}^*)y_\tau I^*e^{-\mu_3\tau}\\
&+(\varphi_1x_{1,\tau}S_{11}^*+\varphi_2x_{2,\tau}S_{12}^*+\varphi_1x_{3,\tau}S_{21}^*+\varphi_2x_{4,\tau}S_{22}^*)z_\tau W^*e^{-\mu_3\tau}-\mu_3yI^*-hyI^*]\\
&+a_2\left(1-\frac{1}{z}\right)(kyI^*-dzW^*)\\
&=[A_1+\alpha_1S_{11}^*+\mu_1S_{11}^*+\mu_2S_{12}^*+A_2+\mu_1S_{21}^*+\alpha_2S_{21}^*+\mu_2S_{22}^*+a_1(\mu_3I^*+hI^*)\\
&+a_2dW^*]-\beta_{11}S_{11}^*I^*(x_1y-y)-\varphi_1S_{11}^*W^*(x_1z-z)-\mu_1S_{11}^*x_1-\mu_2S_{12}^*x_2\\
&-A_1\frac{1}{x_1}-\alpha_1\frac{x_1}{x_2}S_{11}^*-\beta_{12}S_{12}^*I^*(x_2y-y)-\varphi_2S_{12}^*W^*(x_2z-z)-\mu_1S_{21}^*x_3\\
&-\beta_{21}S_{21}^*I^*(x_3y-y)-\varphi_1S_{21}^*W^*(x_3z-z)-A_2\frac{1}{x_3}-\alpha_2\frac{x_3}{x_4}S_{21}^*-\mu_2S_{22}^*x_4
\end{aligned}
$$

$$
\begin{aligned}
&- \beta_{22}S^*_{22}I^*(x_4y - y) - \varphi_2 S^*_{22}W^*(x_4z - z)\\
&+ a_1(\beta_{11}S^*_{11}x_{1,\tau} + \beta_{12}S^*_{12}x_{2.\tau} + \beta_{21}S^*_{21}x_{3,\tau} + \beta_{22}S^*_{22}x_{4,\tau})(y_\tau - \frac{y_\tau}{y})I^*e^{-\mu_3\tau}\\
&+ a_1(\varphi_1 S^*_{11}x_{1,\tau} + \varphi_2 S^*_{12}x_{2.\tau} + \varphi_1 S^*_{21}x_{3,\tau} + \varphi_2 S^*_{22}x_{4,\tau})(z_\tau - \frac{z_\tau}{y})W^*e^{-\mu_3\tau}\\
&- a_1(\mu_3 I^* y + hyI^*) + a_2(kyI^* - dW^*z) - a_2k\frac{y}{z}I^*.
\end{aligned}
$$

Denote

$$
\begin{aligned}
H_0 \equiv\ & - \beta_{11}S^*_{11}y^*(\ln x_1y - \ln y) - \varphi_1 S^*_{11}W^*(\ln x_1z - \ln z) - \mu_1 S^*_{11}\ln x_1\\
&- \mu_2 S^*_{12}\ln x_2 - A_1\ln\frac{1}{x_1} - \alpha_1 S^*_{11}\ln\frac{x_1}{x_2} - \beta_{12}S^*_{12}I^*(\ln x_2y - \ln y)\\
&- \varphi_2 S^*_{12}W^*(\ln x_2z - \ln z) - \mu_1 S^*_{21}\ln x_3 - \beta_{21}S^*_{21}I^*(\ln x_3y - \ln y)\\
&- \varphi_1 S^*_{21}W^*(\ln x_3z - \ln z) - A_2\ln\frac{1}{x_3} - \alpha_2 S^*_{21}\ln\frac{x_3}{x_4} - \mu_2 S^*_{22}\ln x_4\\
&- \beta_{22}S^*_{22}I^*(\ln x_4y - \ln y) - \varphi_2 S^*_{22}W^*(\ln x_4z - \ln z)\\
&+ a_1(\beta_{11}S^*_{11}\ln x_{1,\tau}y_\tau + \beta_{12}S^*_{12}\ln x_{2,\tau}y_\tau + \beta_{21}S^*_{21}\ln x_{3,\tau}y_\tau + \beta_{22}S^*_{22}\ln x_{4,\tau}y_\tau)I^*e^{-\mu_3\tau}\\
&- a_1(\beta_{11}S^*_{11}\ln x_{1,\tau}\frac{y_\tau}{y} + \beta_{12}S^*_{12}\ln x_{2,\tau}\frac{y_\tau}{y} + \beta_{21}S^*_{21}\ln x_{3,\tau}\frac{y_\tau}{y} + \beta_{22}S^*_{22}\ln x_{4,\tau}\frac{y_\tau}{y})I^*e^{-\mu_3\tau}\\
&+ a_1(\varphi_1 S^*_{11}\ln x_{1,\tau}z_\tau + \varphi_2 S^*_{12}\ln x_{2,\tau}z_\tau + \varphi_1 S^*_{21}\ln x_{3,\tau}z_\tau + \varphi_2 S^*_{22}\ln x_{4,\tau}z_\tau)W^*e^{-\mu_3\tau}\\
&- a_1(\varphi_1 S^*_{11}\ln x_{1,\tau}\frac{z_\tau}{y} + \varphi_2 S^*_{12}\ln x_{2,\tau}\frac{z_\tau}{y} + \varphi_1 S^*_{21}\ln x_{3,\tau}\frac{z_\tau}{y} + \varphi_2 S^*_{22}\ln x_{4,\tau}\frac{z_\tau}{y})W^*e^{-\mu_3\tau}\\
&- a_1\mu_3 I^*\ln y - a_1hI^*\ln y + a_2kI^*\ln y - a_2dW^*\ln z - a_2kI^*\ln\frac{y}{z}.
\end{aligned}
$$

Obviously, $H_0 \equiv 0$. Therefore,

$$
\begin{aligned}
\frac{\mathrm{d}V_2}{\mathrm{d}t} &= \frac{\mathrm{d}V_2}{\mathrm{d}t} - H_0\\
&= - A_1g(\frac{1}{x_1}) - \alpha_1 S^*_{11}g(\frac{x_1}{x_2}) - \mu_1 S^*_{11}g(x_1) - \mu_2 S^*_{12}g(x_2) - A_2g(\frac{1}{x_3}) - \mu_1 S^*_{21}g(x_3)\\
&\quad - \alpha_2 S^*_{21}g(\frac{x_3}{x_4}) - \mu_2 S^*_{22}g(x_4) - a_1(\mu_3 I^* + hI^*)g(y) - a_2dW^*g(z) - \beta_{11}S^*_{11}I^*g(x_1y)\\
&\quad + \beta_{11}S^*_{11}I^*g(y) - \varphi_1 S^*_{11}W^*g(x_1z) + \varphi_1 S^*_{11}W^*g(z) - \beta_{12}S^*_{12}I^*g(x_2y)\\
&\quad + \beta_{12}S^*_{12}I^*g(y) - \varphi_2 S^*_{12}W^*g(x_2z) + \varphi_2 S^*_{12}W^*g(z) - \beta_{21}S^*_{21}I^*g(x_3y)\\
&\quad + \beta_{21}S^*_{21}I^*g(y) - \varphi_1 S^*_{21}W^*g(x_3z) + \varphi_1 S^*_{21}W^*g(z) - \beta_{22}S^*_{22}I^*g(x_4y)\\
&\quad + \beta_{22}S^*_{22}I^*g(y) - \varphi_2 S^*_{22}W^*g(x_4z) + \varphi_2 S^*_{22}W^*g(z)\\
&\quad + a_1I^*e^{-\mu_3\tau}\Big\{\beta_{11}S^*_{11}\Big[g(x_{1,\tau}y_\tau) - g\Big(\frac{x_{1,\tau}y_\tau}{y}\Big)\Big] + \beta_{12}S^*_{12}\Big[g(x_{2,\tau}y_\tau) - g\Big(\frac{x_{2,\tau}y_\tau}{y}\Big)\Big]\\
&\quad + \beta_{21}S^*_{21}\Big[g(x_{3,\tau}y_\tau) - g\Big(\frac{x_{3,\tau}y_\tau}{y}\Big)\Big] + \beta_{22}S^*_{22}\Big[g(x_{4,\tau}y_\tau) - g\Big(\frac{x_{4,\tau}y_\tau}{y}\Big)\Big]\Big\}\\
&\quad + a_1W^*e^{-\mu_3\tau}\Big\{\varphi_1 S^*_{11}\Big[g(x_{1,\tau}z_\tau) - g\Big(\frac{x_{1,\tau}z_\tau}{y}\Big)\Big] + \varphi_2 S^*_{12}\Big[g(x_{2,\tau}z_\tau) - g\Big(\frac{x_{2,\tau}z_\tau}{y}\Big)\Big]
\end{aligned}
$$

$$+\varphi_1 S_{21}^*\Big[g(x_{3,\tau}z_\tau)-g\Big(\frac{x_{3,\tau}y_\tau}{y}\Big)\Big]+\varphi_2 S_{22}^*\Big[g(x_{4,\tau}z_\tau)-g\Big(\frac{x_{4,\tau}z_\tau}{y}\Big)\Big]\Big\}$$
$$+a_2kI^*g(y)-a_2kI^*g\Big(\frac{y}{z}\Big).$$

Define the Lyapunov functional

$$\begin{aligned}V=V_2&+\beta_{11}\int_{t-\tau}^{t}S_{11}^*I^*g\Big(\frac{S_{11}(\theta)I(\theta)}{S_{11}^*I^*}\Big)d\theta+\beta_{12}\int_{t-\tau}^{t}S_{12}^*I^*g\Big(\frac{S_{12}(\theta)I(\theta)}{S_{12}^*I^*}\Big)d\theta\\&+\beta_{21}\int_{t-\tau}^{t}S_{21}^*I^*g\Big(\frac{S_{21}(\theta)I(\theta)}{S_{21}^*I^*}\Big)d\theta+\beta_{22}\int_{t-\tau}^{t}S_{22}^*I^*g\Big(\frac{S_{22}(\theta)I(\theta)}{S_{22}^*I^*}\Big)d\theta\\&+\varphi_1\int_{t-\tau}^{t}S_{11}^*W^*g\Big(\frac{S_{11}(\theta)W(\theta)}{S_{11}^*W^*}\Big)+\varphi_2\int_{t-\tau}^{t}S_{12}^*W^*g\Big(\frac{S_{12}(\theta)W(\theta)}{S_{12}^*W^*}\Big)\\&+\varphi_1\int_{t-\tau}^{t}S_{21}^*W^*g\Big(\frac{S_{21}(\theta)W(\theta)}{S_{21}^*W^*}\Big)+\varphi_2\int_{t-\tau}^{t}S_{22}^*W^*g\Big(\frac{S_{22}(\theta)W(\theta)}{S_{22}^*W^*}\Big).\end{aligned}$$

Thus, we can get

$$\begin{aligned}\frac{\mathrm{d}V}{\mathrm{d}t}=&-A_1g(\frac{1}{x_1})-\alpha_1S_{11}^*g(\frac{x_1}{x_2})-\mu_1S_{11}^*g(x_1)-\mu_2S_{12}^*g(x_2)-A_2g(\frac{1}{x_3})-\mu_1S_{21}^*g(x_3)\\&-\alpha_2S_{21}^*g(\frac{x_3}{x_4})-\mu_2S_{22}^*g(x_4)+[-a_1(\mu_3+h)+\beta_{11}S_{11}^*+\beta_{12}S_{12}^*+\beta_{21}S_{21}^*\\&+\beta_{22}S_{22}^*+a_2k]I^*g(y)+[\varphi_1S_{11}^*+\varphi_2S_{12}^*+\varphi_1S_{21}^*+\varphi_2S_{22}^*-a_2d]W^*g(z)\\&+(a_1e^{-\mu_3\tau}-1)I^*[\beta_{11}S_{11}^*g(x_{1,\tau}y_\tau)+\beta_{12}S_{12}^*g(x_{2,\tau}y_\tau)+\beta_{21}S_{21}^*g(x_{3,\tau}y_\tau)+\beta_{22}S_{22}^*g(x_{4,\tau}y_\tau)]\\&+(a_1e^{-\mu_3\tau}-1)W^*[\varphi_1S_{11}^*g(x_{1,\tau}z_\tau)+\varphi_2S_{12}^*g(x_{2,\tau}z_\tau)+\varphi_1S_{21}^*g(x_{3,\tau}z_\tau)+\varphi_2S_{22}^*g(x_{4,\tau}z_\tau)]\\&-a_1I^*e^{-\mu_3\tau}\Big[\beta_{11}S_{11}^*g\Big(\frac{x_{1,\tau}y_\tau}{y}\Big)+\beta_{12}S_{12}^*g\Big(\frac{x_{2,\tau}y_\tau}{y}\Big)+\beta_{21}S_{21}^*g\Big(\frac{x_{3,\tau}y_\tau}{y}\Big)+\beta_{22}S_{22}^*g\Big(\frac{x_{4,\tau}y_\tau}{y}\Big)\Big]\\&-a_1W^*e^{-\mu_3\tau}\Big[\varphi_1S_{11}^*g\Big(\frac{x_{1,\tau}z_\tau}{y}\Big)+\varphi_2S_{12}^*g\Big(\frac{x_{2,\tau}z_\tau}{y}\Big)+\varphi_1S_{21}^*g\Big(\frac{x_{3,\tau}z_\tau}{y}\Big)+\varphi_2S_{22}^*g\Big(\frac{x_{4,\tau}z_\tau}{y}\Big)\Big]\\&-a_2kI^*g\Big(\frac{y}{z}\Big).\end{aligned}$$

To ensure that $\frac{\mathrm{d}V}{\mathrm{d}t}\le 0$, each coefficient must satisfy the following inequality relations:

$$0\le a_1\le e^{\mu_3\tau},\quad \frac{\varphi_1S_{11}^*+\varphi_2S_{12}^*+\varphi_1S_{21}^*+\varphi_2S_{22}^*}{d}\le a_2\le b,$$

where $b=\frac{1}{k}[a_1(\mu_3+h)-(\beta_{11}S_{11}^*+\beta_{12}S_{12}^*+\beta_{21}S_{21}^*+\beta_{22}S_{22}^*)]$. So, we can obtain $a_1=e^{\mu_3\tau}, a_2=\frac{\varphi_1S_{11}^*+\varphi_2S_{12}^*+\varphi_1S_{21}^*+\varphi_2S_{22}^*}{d}$. With this choice, we have

$$\begin{aligned}V=&S_{11}^*g\left(\frac{S_{11}}{S_{11}^*}\right)+S_{12}^*g\left(\frac{S_{12}}{S_{12}^*}\right)+S_{21}^*g\left(\frac{S_{21}}{S_{21}^*}\right)+S_{22}^*g\left(\frac{S_{22}}{S_{22}^*}\right)+e^{\mu_3\tau}I^*g\left(\frac{I}{I^*}\right)\\&+\frac{\varphi_1S_{11}^*+\varphi_2S_{12}^*+\varphi_1S_{21}^*+\varphi_2S_{22}^*}{d}W^*g\left(\frac{W}{W^*}\right)\\&+\beta_{11}\int_{t-\tau}^{t}S_{11}^*I^*g\Big(\frac{S_{11}(\theta)I(\theta)}{S_{11}^*I^*}\Big)d\theta+\beta_{12}\int_{t-\tau}^{t}S_{12}^*I^*g\Big(\frac{S_{12}(\theta)I(\theta)}{S_{12}^*I^*}\Big)d\theta\end{aligned}$$

$$
\begin{aligned}
&+\beta_{21}\int_{t-\tau}^{t} S_{21}^{*}I^{*}g\Big(\frac{S_{21}(\theta)I(\theta)}{S_{21}^{*}I^{*}}\Big)d\theta+\beta_{22}\int_{t-\tau}^{t} S_{22}^{*}I^{*}g\Big(\frac{S_{22}(\theta)I(\theta)}{S_{22}^{*}I^{*}}\Big)d\theta\\
&+\varphi_1\int_{t-\tau}^{t} S_{11}^{*}W^{*}g\Big(\frac{S_{11}(\theta)W(\theta)}{S_{11}^{*}W^{*}}\Big)+\varphi_2\int_{t-\tau}^{t} S_{12}^{*}W^{*}g\Big(\frac{S_{12}(\theta)W(\theta)}{S_{12}^{*}W^{*}}\Big)\\
&+\varphi_1\int_{t-\tau}^{t} S_{21}^{*}W^{*}g\Big(\frac{S_{21}(\theta)W(\theta)}{S_{21}^{*}W^{*}}\Big)+\varphi_2\int_{t-\tau}^{t} S_{22}^{*}W^{*}g\Big(\frac{S_{22}(\theta)W(\theta)}{S_{22}^{*}W^{*}}\Big)
\end{aligned}
\tag{4.5}
$$

and

$$
\begin{aligned}
\frac{\mathrm{d}V}{\mathrm{d}t} = &-A_1g(\frac{1}{x_1})-\alpha_1S_{11}^{*}g(\frac{x_1}{x_2})-\mu_1S_{11}^{*}g(x_1)-\mu_2S_{12}^{*}g(x_2)-A_2g(\frac{1}{x_3})-\mu_1S_{21}^{*}g(x_3)\\
&-\alpha_2S_{21}^{*}g(\frac{x_3}{x_4})-\mu_2S_{22}^{*}g(x_4)-\frac{\varphi_1S_{11}^{*}+\varphi_2S_{12}^{*}+\varphi_1S_{21}^{*}+\varphi_2S_{22}^{*}}{d}kI^{*}g\Big(\frac{y}{z}\Big)\\
&-I^{*}\Big[\beta_{11}S_{11}^{*}g\Big(\frac{x_{1,\tau}y_\tau}{y}\Big)+\beta_{12}S_{12}^{*}g\Big(\frac{x_{2,\tau}y_\tau}{y}\Big)+\beta_{21}S_{21}^{*}g\Big(\frac{x_{3,\tau}y_\tau}{y}\Big)+\beta_{22}S_{22}^{*}g\Big(\frac{x_{4,\tau}y_\tau}{y}\Big)\Big]\\
&-W^{*}\Big[\varphi_1S_{11}^{*}g\Big(\frac{x_{1,\tau}z_\tau}{y}\Big)+\varphi_2S_{12}^{*}g\Big(\frac{x_{2,\tau}z_\tau}{y}\Big)+\varphi_1S_{21}^{*}g\Big(\frac{x_{3,\tau}z_\tau}{y}\Big)+\varphi_2S_{22}^{*}g\Big(\frac{x_{4,\tau}z_\tau}{y}\Big)\Big].
\end{aligned}
$$

Therefore, $\frac{\mathrm{d}V}{\mathrm{d}t}\le 0$ and $\frac{\mathrm{d}V}{\mathrm{d}t}=0$ if and only if $x_1=x_2=x_3=x_4=1$ and $\frac{y}{z}=1$, which means $\frac{S_{11}}{S_{11}^{*}}=\frac{S_{12}}{S_{12}^{*}}=\frac{S_{21}}{S_{21}^{*}}=\frac{S_{22}}{S_{22}^{*}}=1$ and $\frac{IW^{*}}{I^{*}W}=1$. It can then be easily verified that the maximal invariant set within the set where $\frac{\mathrm{d}V}{\mathrm{d}t}=0$ is the singleton set $\{P^{*}\}$. According to LaSalle's invariance principle, the endemic equilibrium $P^{*}$ is globally asymptotically stable when $\mathscr{R}_0>1$.

## 5. Target reproduction number and its applications

In this section, we will employ the target reproduction number to evaluate the control effects of different measures on brucellosis.

### *5.1. Target reproduction number*

The time-delayed target reproduction number represents an important extension of the classical target reproduction number to time-delayed models. Its core concept lies in incorporating time delay effects, such as incubation and maturation periods, into the processes of new infection generation, population internal evolution, and state transitions. By addressing the limitation of classical approaches that neglect time delays, this framework enables precise assessment of control strategy effectiveness in delayed systems, thereby providing systematic theoretical foundations and practical guidance for targeted interventions in epidemiology, ecology, and related fields.

The basic reproduction number is given by the spectral radius of the next generation matrix: $\mathscr{R}_0=\rho(\hat{\boldsymbol{F}}\hat{\boldsymbol{V}}^{-1})$, where $\hat{\boldsymbol{F}}$ is to capture the new infection and $\hat{\boldsymbol{V}}$ is to describe internal transitions within the infected compartments. According to Reference [25], define $\mathcal{L}=\hat{\boldsymbol{F}}\hat{\boldsymbol{V}}^{-1}=\mathcal{M}+\mathcal{N}$, where $\mathcal{M}$ is a target operator satisfying $0\le\mathcal{M}\le\mathcal{L}$ and $\mathcal{N}$ is a non-target operator. If $\rho(\mathcal{N})<1$, the target reproduction number associated with $\mathcal{M}$ is defined as

$$
T_{\mathcal{M}}=\rho\left(\mathcal{M}(\boldsymbol{I}-\mathcal{N})^{-1}\right). \tag{5.1}
$$

The explicit formulas for computing the time-delayed target reproduction number are given as follows:

**(i) The control objective is new infection**.

Let $S \subset \{1, \cdots, m\} \times \{1, \cdots, m\}$ denote a given target set. The new infection matrix is decomposed as

$$\hat{\boldsymbol{F}} = \hat{\boldsymbol{F}}_S + (\hat{\boldsymbol{F}} - \hat{\boldsymbol{F}}_S),$$

where $\hat{\boldsymbol{F}}_S$ is the matrix containing only the elements of $\hat{\boldsymbol{F}}$ whose indices belong to $S$, with all other elements set to zero. If $\rho\left(\left(\hat{\boldsymbol{F}} - \hat{\boldsymbol{F}}_S\right)\hat{\boldsymbol{V}}^{-1}\right) < 1$, substituting $\mathcal{M} = \hat{\boldsymbol{F}}_S\hat{\boldsymbol{V}}^{-1}$ and $\mathcal{N} = (\hat{\boldsymbol{F}} - \hat{\boldsymbol{F}}_S)\hat{\boldsymbol{V}}^{-1}$ into (5.1) yields the time-delayed target reproduction number as

$$\mathcal{T}_S = \rho(\hat{\boldsymbol{F}}_S(\hat{\boldsymbol{V}} - (\hat{\boldsymbol{F}} - \hat{\boldsymbol{F}}_S))^{-1}). \tag{5.2}$$

**(ii) The control objective is internal transition**.

When $\hat{\boldsymbol{V}}$ is adjusted by controlling its entries located in the target set $S$, the inverse matrix $\hat{\boldsymbol{V}}^{-1}$ will be correspondingly altered. $C = C(S, \hat{\boldsymbol{V}}) \subset \{1, \cdots, m\} \times \{1, \cdots, m\}$ denotes the corresponding index set that encompasses all indices in $\hat{\boldsymbol{V}}^{-1}$ affected by this adjustment. The matrix $\boldsymbol{B} = (\hat{\boldsymbol{V}}^{-1})_C$ consists exclusively of the elements of $\hat{\boldsymbol{V}}^{-1}$ whose indices belong to $C$ (with all other elements set to zero), where both $\hat{\boldsymbol{V}}^{-1}$ and $\boldsymbol{B}$ are positive linear operators satisfying the inequality $\boldsymbol{B} \leq \hat{\boldsymbol{V}}^{-1}$. If $\rho\left(\hat{\boldsymbol{F}}\left(\hat{\boldsymbol{V}}^{-1} - \boldsymbol{B}\right)\right) < 1$, substituting $\mathcal{M} = \hat{\boldsymbol{F}}\boldsymbol{B}$ and $\mathcal{N} = \hat{\boldsymbol{F}}(\hat{\boldsymbol{V}}^{-1} - \boldsymbol{B})$ into (5.1), the time-delayed target reproduction number is defined as

$$\mathcal{T}_S = \rho\left(\hat{\boldsymbol{F}}\boldsymbol{B}\left(\boldsymbol{I} - \hat{\boldsymbol{F}}\left(\hat{\boldsymbol{V}}^{-1} - \boldsymbol{B}\right)\right)^{-1}\right). \tag{5.3}$$

### *5.2. Applications of target reproduction number in brucellosis control*

In this subsection, we conducte a quantitative evaluation of the effects of three common brucellosis control measures using the target reproduction number: vaccinating the susceptible sheep, isolating the infected sheep, and disinfecting the environment.

For model (4.1),

$$\hat{\boldsymbol{F}} = \begin{bmatrix} f_1 e^{-\mu_3\tau} & f_2 e^{-\mu_3\tau} \\ k & 0 \end{bmatrix}, \quad \hat{\boldsymbol{V}} = \begin{bmatrix} \mu_3 + h & 0 \\ 0 & d \end{bmatrix}.$$

The target reproduction numbers for the above three control measures are computed as follows.

#### 5.2.1. Vaccination

Vaccination reduces the risk of susceptible sheep acquiring brucellosis through direct contact with infected sheep or indirect exposure to contaminated environment. In this context, the first row of $\hat{\boldsymbol{F}}$ represents the incidence of new infections among sheep. Therefore, the target set is $S = \{(1, 1), (1, 2)\}$. By (5.2), we can know the target reproduction number of vaccination is

$$\begin{aligned} \mathcal{T}_1 &= \rho(\hat{\boldsymbol{F}}_S(\hat{\boldsymbol{V}} - (\hat{\boldsymbol{F}} - \hat{\boldsymbol{F}}_S))^{-1}) \\ &= \rho(\hat{\boldsymbol{F}}_S\boldsymbol{G}_1^{-1}) \\ &= \frac{f_1}{\mu_3 + h}e^{-\mu_3\tau} + \frac{kf_2}{d(\mu_3 + h)}e^{-\mu_3\tau}, \end{aligned} \tag{5.4}$$

where

$$\hat{\boldsymbol{F}}_S = \begin{bmatrix} f_1 e^{-\mu_3\tau} & f_2 e^{-\mu_3\tau} \\ 0 & 0 \end{bmatrix}, \quad \boldsymbol{G}_1 = \begin{bmatrix} \mu_3 + h & 0 \\ -k & d \end{bmatrix}.$$

Let ram-to-ewe ratio $m = \frac{S^0_{12}}{S^0_{22}}$. For a given vaccine supply, vaccination can be administered by age or sex. Using these relations and (5.4), the target reproduction numbers for both strategies are given by:

**(i) Age-based vaccination**: the target reproduction number for age-based vaccination is expressed as

$$\mathcal{T}_a = \frac{d\mu_2\beta_{11}m\alpha_2 + k\mu_2\varphi_1 m\alpha_2 + d\mu_2\beta_{21}\alpha_1 + k\mu_2\varphi_1\alpha_1}{\Theta}\mathcal{T}_L + \frac{d\beta_{12}m\alpha_1\alpha_2 + k\varphi_2 m\alpha_1\alpha_2 + d\beta_{22}\alpha_1\alpha_2 + k\varphi_2\alpha_1\alpha_2}{\Theta}\mathcal{T}_A,$$

where $\Theta = d(\mu_2\beta_{11}m\alpha_2+\beta_{12}\alpha_1\alpha_2 m+\alpha_1\mu_2\beta_{21}+\beta_{22}\alpha_1\alpha_2)+k(\mu_2\varphi_1 m\alpha_2+m\varphi_2\alpha_1\alpha_2+\mu_2\varphi_1\alpha_1+\varphi_2\alpha_1\alpha_2)$, $\mathcal{T}_L$ and $\mathcal{T}_A$ denote the target reproduction numbers for vaccinating only lambs and adult sheep, respectively, and are given by

$$\mathcal{T}_L = \frac{d\mu_2\beta_{11} + d\alpha_1\beta_{12} + k\mu_2\varphi_1 + k\varphi_2\alpha_1}{d\mu_2(\mu_3 + h)}e^{-\mu_3\tau}S^0_{11} + \frac{d\mu_2\beta_{21} + d\alpha_2\beta_{22} + k\mu_2\varphi_1 + k\alpha_2\varphi_2}{d\mu_2(\mu_3 + h)}e^{-\mu_3\tau}S^0_{21},$$

$$\mathcal{T}_A = \frac{d\beta_{11}\mu_2 + d\beta_{12}\alpha_1 + k\varphi_1\mu_2 + k\alpha_1\varphi_2}{d\alpha_1(\mu_3 + h)}e^{-\mu_3\tau}S^0_{12} + \frac{d\beta_{21}\mu_2 + d\alpha_2\beta_{22} + k\varphi_1\mu_2 + k\alpha_2\varphi_2}{d\alpha_2(\mu_3 + h)}e^{-\mu_3\tau}S^0_{22}.$$

**(ii) Sex-based vaccination**: the target reproduction number for sex-based vaccination is expressed as

$$\mathcal{T}_s = \frac{d\mu_2\beta_{11}m\alpha_2 + k\mu_2\varphi_1 m\alpha_2 + d\beta_{12}m\alpha_1\alpha_2 + k\varphi_2 m\alpha_1\alpha_2}{\Theta}\mathcal{T}_r + \frac{d\mu_2\alpha_1\beta_{21} + k\mu_2\varphi_1\alpha_1 + d\alpha_1\alpha_2\beta_{22} + k\alpha_1\alpha_2\varphi_2}{\Theta}\mathcal{T}_e,$$

where $\mathcal{T}_r$ and $\mathcal{T}_e$ represent the target reproduction numbers for vaccinating only rams and ewes, respectively, and are given by

$$\mathcal{T}_r = \frac{d\mu_2\beta_{11} + d\alpha_1\beta_{12} + k\varphi_1\mu_2 + k\alpha_1\varphi_2}{d\mu_2(\mu_3 + h)}e^{-\mu_3\tau}S^0_{11} + \frac{d\beta_{21}\mu_2 + d\alpha_2\beta_{22} + k\mu_2\varphi_1 + k\varphi_2\alpha_2}{dm\alpha_2(\mu_3 + h)}e^{-\mu_3\tau}S^0_{12},$$

$$\mathcal{T}_e = \frac{m\alpha_2(d\beta_{11}\mu_2 + d\beta_{12}\alpha_1 + k\varphi_1\mu_2 + k\alpha_1\varphi_2)}{d\alpha_1\mu_2(\mu_3 + h)}e^{-\mu_3\tau}S^0_{21} + \frac{d\beta_{21}\mu_2 + d\alpha_2\beta_{22} + k\varphi_1\mu_2 + k\alpha_2\varphi_2}{d\alpha_2(\mu_3 + h)}e^{-\mu_3\tau}S^0_{22}.$$

5.2.2. Isolation

Isolating the infected sheep is a key strategy for reducing direct contact; therefore, the target set is $S = \{(1, 1)\}$. Using (5.2), the target reproduction number of isolation is

$$\begin{aligned}\mathcal{T}_2 &= \rho(\hat{\boldsymbol{F}}_S(\hat{\boldsymbol{V}} - (\hat{\boldsymbol{F}} - \hat{\boldsymbol{F}}_S))^{-1}) \\ &= \rho(\hat{\boldsymbol{F}}_S \boldsymbol{G}_2^{-1}) \\ &= \frac{1}{\mu_3 + h} \cdot \frac{f_1 e^{-\mu_3 \tau}}{1 - \frac{k f_2}{d(\mu_3+h)} e^{-\mu_3 \tau}},\end{aligned} \tag{5.5}$$

where

$$\hat{\boldsymbol{F}}_s = \begin{bmatrix} f_1 e^{-\mu_3 \tau} & 0 \\ 0 & 0 \end{bmatrix}, \quad \boldsymbol{G}_2 = \begin{bmatrix} \mu_3 + h & -f_2 e^{-\mu_3 \tau} \\ -k & d \end{bmatrix}.$$

5.2.3. Disinfection

Disinfection refers to the reduction of Brucella pathogen load in the environment. Correspondingly, the element in the second row and second column of matrix $\hat{\boldsymbol{V}}$ represents the removal rate of Brucella from the environment. Therefore, the target set is defined as $S = \{(2, 2)\}$. Using the formula (5.3), we obtain the target reproduction number for environmental disinfection as follows:

$$\mathcal{T}_3 = \frac{1}{d(\mu_3 + h)} \cdot \frac{k f_2 e^{-\mu_3 \tau}}{1 - \frac{f_1}{\mu_3+h} e^{-\mu_3 \tau}}. \tag{5.6}$$

Combining Theorem 2.1 in [26] and Corollary 5.1 in [27], the following conclusions can be easily obtained.

**Corollary 5.1.** *Suppose that* $\hat{\boldsymbol{F}}\hat{\boldsymbol{V}}^{-1}$ *is irreducible,* $\rho\left(\left(\hat{\boldsymbol{F}} - \hat{\boldsymbol{F}}_S\right)\hat{\boldsymbol{V}}^{-1}\right) < 1$ *or* $\rho\left(\hat{\boldsymbol{F}}\left(\hat{\boldsymbol{V}}^{-1} - \boldsymbol{B}\right)\right) < 1$*, then*

*(i) The disease-free equilibrium* $P^0$ *is globally asymptotically stable in* $\Gamma$ *when* $\mathcal{T} < 1$*,*
*(ii) The endemic equilibrium* $P^*$ *is globally asymptotically stable in* $\text{int}(\Gamma)$ *when* $\mathcal{T} > 1$*.*

*Here,* $\mathcal{T}$ *denotes any one of* $\mathcal{T}_i$ $(i = 1, 2, 3)$*.*

## 6. Numerical simulations and analysis of control measures

In this section, we first evaluate the stability of the equilibria of model (4.1) through numerical simulations, and examine the impact of time delay $\tau$ on the number of infected sheep $I$ and Brucella load $W$ in the environment. We then investigate how time delay $\tau$ influences the target reproduction number, and assess the effectiveness of three control measures (i.e., vaccination, isolation, and disinfection) based on the target reproduction number. Finally, we analyze the cost-effectiveness of age-structured and sex-structured vaccination strategies under various scenarios.

### *6.1. Stability analysis of equilibria in model* (4.1) *and the impact of* $\tau$ *on infected sheep and Brucella*

6.1.1. The stability of equilibria for model (4.1)

The initial values of model (4.1) are set as $S_{11}(0) = 900, S_{12}(0) = 1600, S_{21}(0) = 1200, S_{22}(0) = 2420, I(0) = 61$, and $W(0) = 127$. The parameter values of model (4.1) are adopted from [6, 7, 10]:

$\alpha_1 = 1.06, \alpha_2 = 1.06, k = 15, d = 3.577, \mu_1 = 0.1, \mu_2 = 0.25, \mu_3 = 0.25, h = 0.15, \varphi_1 = 5.4 \times 10^{-6}, \varphi_2 = 1.35 \times 10^{-5}, \beta_{11} = \beta_{21} = 1.52 \times 10^{-5}, \beta_{12} = 2.15 \times 10^{-5}$, and $\beta_{22} = 4.57 \times 10^{-5}$. The time delay is set to $\tau = 0.05$ year.

To begin with, it can be calculated that $\mathscr{R}_0 = 0.6372 < 1$ when $A_1 = 300, A_2 = 400$. As shown in Figure 2(a), the solution $(S_{11}, S_{12}, S_{21}, S_{22}, I, W)$ converges to $P^0 \approx (258, 1096, 344, 1462, 0, 0)$ as time progresses, indicating that the disease-free equilibrium $P^0$ of model (4.1) is globally asymptotically stable. This result is consistent with Theorem 4.1. Next, keeping all other parameters fixed, we obtain $\mathscr{R}_0 = 1.3747 > 1$ when $A_1 = 600, A_2 = 900$. As illustrated in Figure 2(b), the solution approaches the unique endemic equilibrium $P^* \approx (500, 1617, 751, 2259, 1000, 4191)$ as time evolves, verifying the globally asymptotic stability of $P^*$. This result is in perfect agreement with Theorem 4.2.

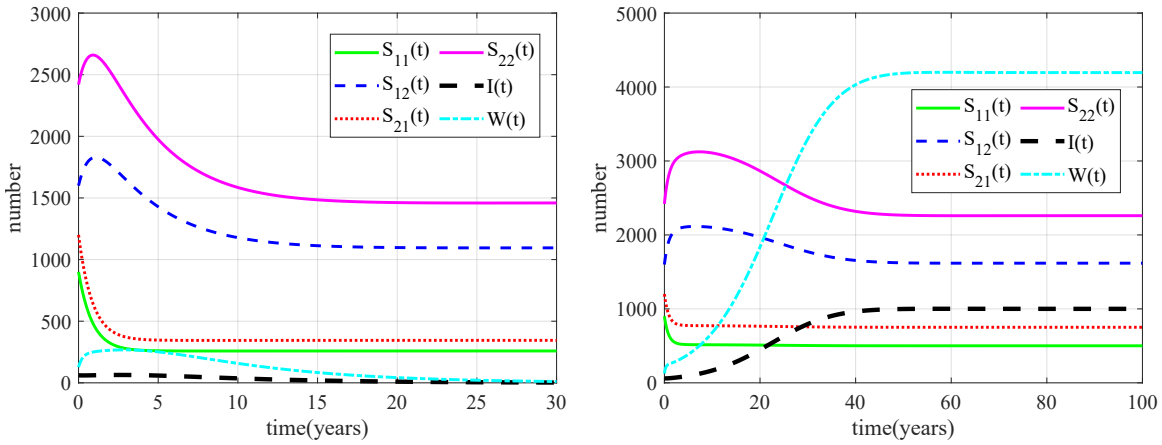


(a) $\mathscr{R}_0 < 1$ (b) $\mathscr{R}_0 > 1$

**Figure 2.** The time series plot of the solutions of model (4.1).

### 6.1.2. The impact of $\tau$ on infected sheep and Brucella

First, Figures 3(a),(b) demonstrate that, regardless of whether $\mathscr{R}_0 < 1$ or $\mathscr{R}_0 > 1$, different time delays $\tau$ do not alter the final epidemic trend of brucellosis. However, a larger $\tau$ leads to a smaller number of infected sheep. Second, the results in Figure 3(c),(d) further indicate that the time delay does not affect the final epidemic trend of brucellosis under all scenarios, while larger $\tau$ corresponds to a relatively lower Brucella load in the environment. These observations collectively suggest that an extended prolonged time delay can mitigate the transmission potential of brucellosis.

## *6.2. Effectiveness of control measures and formulation of vaccination strategies*

In this subsection, we first perform a sensitivity analysis of the basic reproduction number $\mathscr{R}_0$. We then conduct numerical simulations to examine how time delay $\tau$ influences the time-delayed target reproduction number and compare the effectiveness of various control measures by comparing their respective time-delayed target reproduction numbers. Finally, we explore vaccination coverage under different time delays $\tau$, as well as the cost-effectiveness of age-structured versus sex-structured vaccination strategies across different scenarios, characterized by varying lamb sex ratios and time delays.

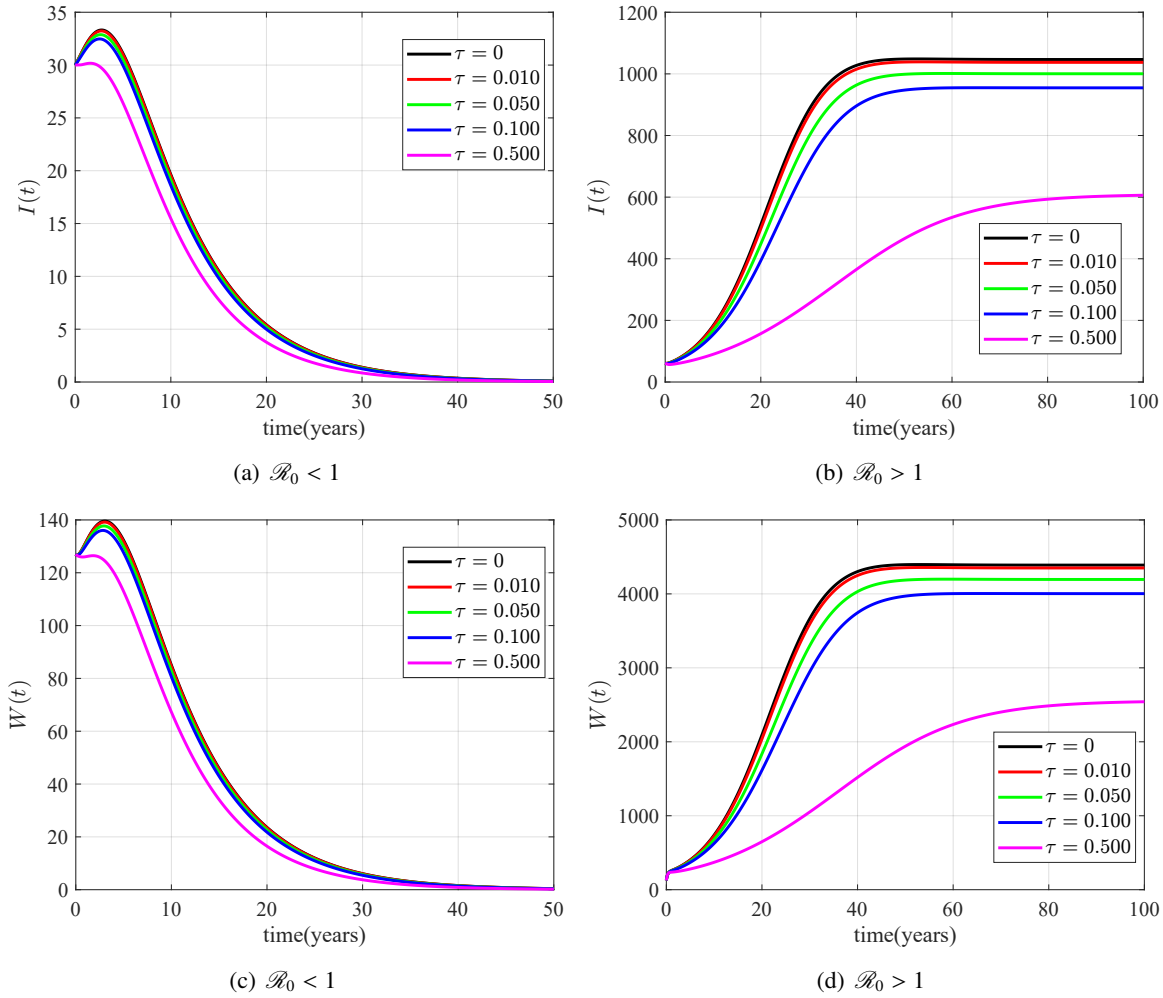


(a) $\mathscr{R}_0 < 1$ (b) $\mathscr{R}_0 > 1$

(c) $\mathscr{R}_0 < 1$ (d) $\mathscr{R}_0 > 1$

**Figure 3.** Variations in the number of sheep and Brucella under different $\tau$ of model (4.1).

6.2.1. Analysis of the effectiveness of control measures

To assess the impact of all model parameters on the transmission of brucellosis, we conduct a sensitivity analysis on the basic reproduction number $\mathscr{R}_0$ using the partial rank correlation coefficient (PRCC) method. From Figure 4, it can be observed that $A_1$, $A_2$, $\beta_{11}$, $\beta_{12}$, $\beta_{21}$, $\beta_{22}$, $\varphi_1$, $\varphi_2$, $\alpha_2$, and $k$ are positively correlated with $\mathscr{R}_0$, while $\alpha_1$, $d$, and $h$ show a negative correlation with $\mathscr{R}_0$. The PRCC values of $\beta_{11}$ and $\beta_{21}$ are significantly smaller than those of $\beta_{12}$ and $\beta_{22}$, indicating that adult sheep play a significant role in brucellosis transmission by age. Additionally, the PRCC values of $\beta_{11}$ and $\beta_{12}$ are smaller than those of $\beta_{21}$ and $\beta_{22}$, suggesting that ewes play a more prominent role with respect to sex. Notably, the PRCC value of $\varphi_2$ is significantly greater than those of $\beta_{11}$, $\beta_{12}$, $\beta_{21}$, and $\beta_{22}$, highlighting that environmental factors also play a crucial role in brucellosis transmission.

Based on the above analysis, we focus on the four parameters that most significantly influence $\mathscr{R}_0$, namely $\varphi_2$, $k$, $d$, and $h$, and investigate how their variation affects the control strategies.

Figure 5 reveals that the time-delayed target reproduction number is inversely related to $\tau$ (i.e., larger $\tau$ values correspond to smaller target reproduction number, thereby reducing the required intensity of control measures). Furthermore, when $\mathcal{T} > 1$, vaccination is the most effective control measure,

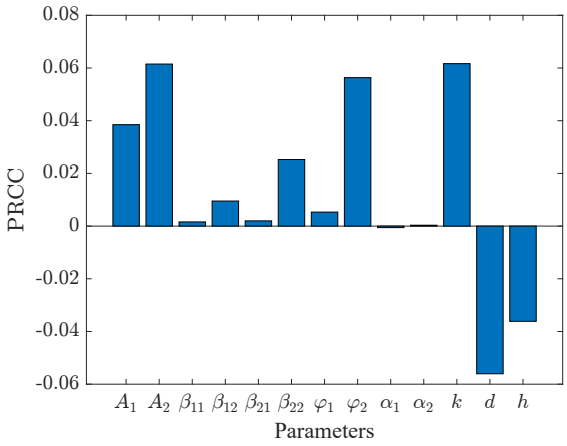


**Figure 4.** Sensitivity analysis of the basic reproduction number $\mathscr{R}_0$.

followed by disinfection, with isolation being the least effective.

6.2.2. Cost analysis of vaccination strategies and plan formulation based on $\tau$

The above studies have shown that vaccination of sheep is a key measure for the prevention and control of brucellosis. In addition, the results in Section 5 indicated that the vaccination rate is independent of time delay. However, does the time delay $\tau$ affect the formulation of the group vaccination strategy? Therefore, this subsection will explore the impact of the time delay $\tau$ on the vaccination coverage and vaccination cost.

From the perspective of vaccination coverage rate $1 - 1/\mathcal{T}_1$, Figure 6 demonstrates that as $\tau$ increases, the required vaccination coverage rate gradually decreases. This phenomenon can be interpreted as follows: a longer incubation period implies delayed disease progression, which effectively reduces the force of infection at any given time, thereby reducing the necessary vaccination coverage to achieve effective disease control. Based on the above coverage rates, further compare the implementation costs of the two vaccination strategies: age-based vaccination and sex-based vaccination, and then formulate the corresponding vaccination plans.

According to reference [28], the S2 vaccine is a commonly used vaccine for the prevention and control of sheep brucellosis. Considering the pregnancy contraindications, adult ewes are administered oral vaccination (with a dose twice that of the injection vaccine), while the rest of sheep are vaccinated by injection. Assuming the unit cost of the vaccine is 1, the cost functions for the two strategies are defined as follows:

$$C_{age} = [a_1(S^*_{11} + S^*_{21}) + a_2(S^*_{12} + 2S^*_{22})](1 - 1/\mathcal{T}_1), \tag{6.1}$$

$$C_{sex} = [b_1(S^*_{11} + S^*_{12}) + b_2(S^*_{21} + 2S^*_{22})](1 - 1/\mathcal{T}_1), \tag{6.2}$$

where $a_i$ and $b_i$ $(i = 1, 2)$ denote the coefficients corresponding to $\mathcal{T}_L$, $\mathcal{T}_A$, $\mathcal{T}_r$, and $\mathcal{T}_e$. For different values of $A_2/A_1$ and $\tau$, the costs of age-based and sex-based vaccination strategies are calculated using Eqs (6.1) and (6.2), with the results presented in Figure 7. Based on these results, the following conclusions are drawn as follows:

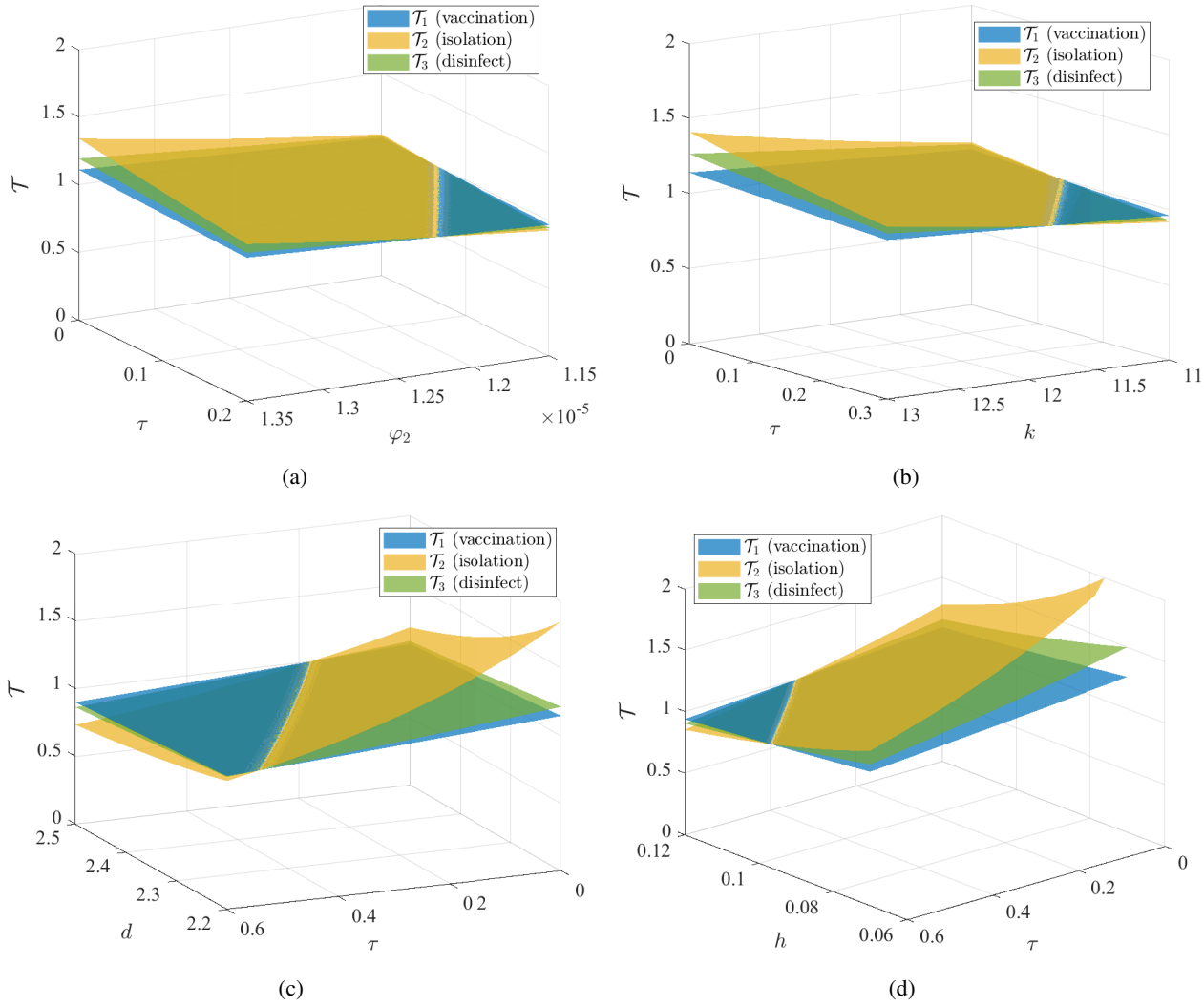


**Figure 5.** Effectiveness of control measures under different parameters.

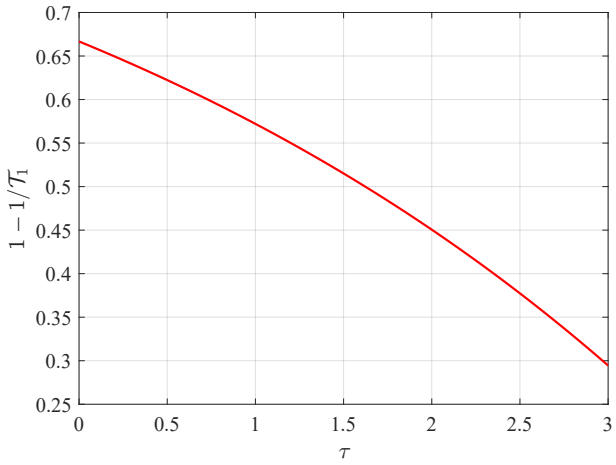


**Figure 6.** Variation of vaccination coverage in the sheep.

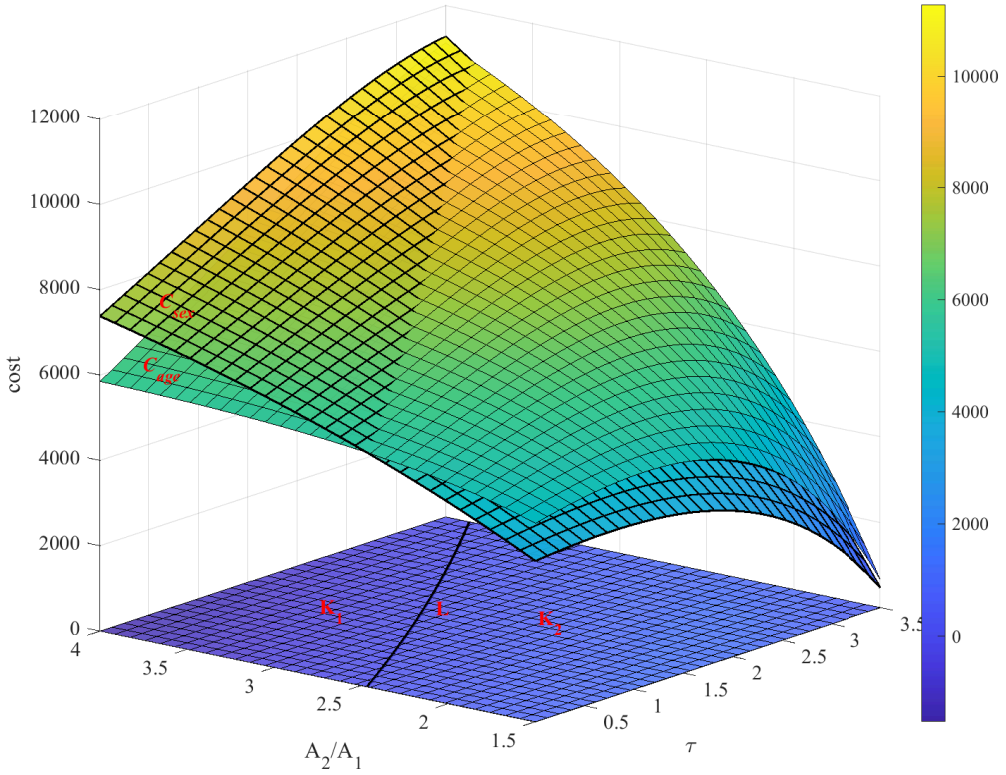


**Figure 7.** Cost of vaccination under different values of $A_2/A_1$ and $\tau$ ($L$ is the intersection line of Regions $K_1$ and $K_2$).

(i) Figure 7 reveals that when the time delay $\tau$ is fixed, the vaccination cost of sheep increases continuously as the ratio $A_2/A_1$ rises. Sex-based vaccination is more cost-effective in region $K_2$, whereas age-based vaccination is more cost-effective in region $K_1$. Additionally, when the ratio $A_2/A_1$ is held constant, the vaccination cost exhibits an overall trend of first increasing and then decreasing as the time delay $\tau$ increases. This is because, during the phase of small $\tau$ variations, the change in vaccination coverage is minimal, while the number of susceptible sheep increases with the rise of $\tau$, resulting in a slight increase in vaccination cost. In contrast, when $\tau$ undergoes large variations, the vaccination coverage is significantly reduced, thereby leading to a decrease in vaccination cost.

(ii) When $A_2/A_1$ and $\tau$ are considered simultaneously, age-based vaccination achieves higher cost-effectiveness if sheep input and time delay $\tau$ fall within region $K_1$, while sex-based vaccination performs better in terms of cost-effectiveness when they lie in region $K_2$.

## 7. Conclusions

Based on the transmission characteristics of sheep brucellosis, this study developed an age-sex structured sheep-environment coupled time-delayed transmission dynamical model. After the stability analysis of the equilibria for model (4.1), we calculated the target reproduction numbers for three con-

trol measures: vaccination, isolation, and disinfection. Numerical simulations revealed that a larger time delay $\tau$ corresponds to a smaller number of infected sheep and Brucella in the environment. Although $\tau$ does not alter the fundamental epidemic trend, the presence of $\tau$ mitigates brucellosis risks by depressing peak infection levels. Subsequently, sensitivity analysis of the basic reproduction number confirmed that the Brucella load in the environment is a key factor in brucellosis transmission, highlighting the importance of indirect transmission routes. During outbreaks, vaccination outperforms isolation and disinfection. Notably, while the vaccination proportion for each subgroup remains invariant with $\tau$, the overall vaccination scope narrows as $\tau$ increases. Finally, based on different values of $A_2/A_1$ and $\tau$, we investigated the cost-effectiveness of age-based and sex-based vaccination strategies: age-based vaccination is preferred in region $K_1$, whereas sex-based vaccination is more economical in region $K_2$.

Given the limitations of this study and existing research gaps, future research directions should focus on developing multi-factor coupled and multi-scale integrated infectious disease models with improved predictive capacity. Specifically, future research should transcend the limitations of ordinary differential equation models in capturing heterogeneity and nonlinear dynamics by exploring coupling mechanisms between socioeconomic factors (e.g., price fluctuations and cross-regional livestock transportation) and biological factors (e.g., environmental pathogen survival and herd immune status), incorporate empirical data (e.g., sheep migration trajectories and environmental monitoring records) to construct intelligent decision-making systems capable of dynamic risk assessment and real-time strategy optimization, and strengthen the application of stochastic dynamics and optimal control theory to quantify uncertainties and identify cost-effective intervention solutions. Ultimately, these efforts will facilitate the transformation of brucellosis prevention from passive response to proactive, precision-based comprehensive management.

## Use of AI tools declaration

The authors declare they have not used Artificial Intelligence (AI) tools in the creation of this article.

## Acknowledgments

This work was jointly supported by the National Natural Science Foundation of China under Grant Nos. 12302017 and 12201330, and the Ningxia Natural Science Foundation Project under Grant Nos. 2024AAC03001 and 2025AAC030001.

## Conflict of interest

The authors declare there is no conflicts of interest.

## References

1. A. R. Khairullah, S. C. Kurniawan, Y. Puspitasari, S. Aryaloka, O. S. M. Silaen, S. M. Yanestria, et al., Brucellosis: Unveiling the complexities of a pervasive zoonotic disease and its global impacts, *Open Vet. J.*, **14** (2024), 1081–1097. https://doi.org/10.5455/OVJ.2024.v14.i5.1

2. Q. Hou, X. Sun, J. Zhang, Y. Liu, Y. Wang, Z. Jin, Modeling the transmission dynamics of sheep brucellosis in Inner Mongolia Autonomous Region, China, *Math. Biosci.*, **242** (2013), 51–58. https://doi.org/10.1016/j.mbs.2012.11.012

3. S. Bai, B. Cao, T. Kang, Q. Wang, A two-stage sheep-environment coupled brucellosis transmission dynamic model: stability analysis and optimal control, *Discrete Contin. Dyn. Syst.-B*, **30** (2025), 1207–1231. https://doi.org/10.3934/dcdsb.2024126

4. J. Megid, L. A. Mathias, C. A. Robles, Clinical manifestations of brucellosis in domestic animals and humans, *Open Vet. Sci. J.*, **4** (2010), 119–126. https://doi.org/10.2174/1874318801004010119

5. G. Sun, M. Li, J. Zhang, W. Zhang, X. Pei, Z. Jin, Transmission dynamics of brucellosis: Mathematical modelling and applications in China, *Comput. Struct. Biotechnol. J.*, **18** (2020), 3843–3860. https://doi.org/10.1016/j.csbj.2020.11.014

6. W. Gong, P. Sun, C. Zhai, J. Yuan, Y. Chen, Q. Chen, et al., Accessibility of the three-year comprehensive prevention and control of brucellosis in Ningxia: A mathematical modeling study, *BMC Infect. Dis.*, **23** (2023), 292. https://doi.org/10.1186/s12879-023-08270-4

7. J. Yang, T. Kang, Q. Wang, The role of age and sex in brucellosis control: insight from the target reproduction number, *Discrete Contin. Dyn. Syst.-B*, (2026), In press. https://doi.org/10.3934/dcdsb.2026023

8. M. Li, G. Sun, J. Zhang, Z. Jin, X. Sun, Y. Wang, et al., Transmission dynamics and control for a brucellosis model in Hinggan League of Inner Mongolia, China, *Math. Biosci. Eng.*, **11** (2014), 1115–1137. https://doi.org/10.3934/mbe.2014.11.1115

9. X. Ma, G. Sun, Global dynamics of a periodic brucellosis model with time delay and environmental factors, *Appl. Math. Modell.*, **130** (2024), 288–309. https://doi.org/10.1016/j.apm.2024.03.002

10. Q. Hou, X. Sun, Modeling sheep brucellosis transmission with a multi-stage model in Changling County of Jilin Province, China, *J. Appl. Math. Comput.*, **51** (2016), 227–244. https://doi.org/10.1007/s12190-015-0901-y

11. S. Bai, B. Cao, T. Kang, Q. Wang, A two-stage sheep brucellosis transmission dynamic model in a patchy environment: Stability analysis and optimization of transportation scheme, *J. Math. Anal. Appl.*, **555** (2025), 130026. https://doi.org/10.1016/j.jmaa.2025.130026

12. M. Li, Z. Shuai, C. Wang, Global stability of multi-group epidemic models with distributed delays, *J. Math. Anal. Appl.*, **361** (2010), 38–47. https://doi.org/10.1016/j.jmaa.2009.09.017

13. H. Shu, D. Fan, J. Wei, Global stability of multi-group SEIR epidemic models with distributed delays and nonlinear transmission, *Nonlinear Anal. Real World Appl.*, **13** (2012), 1581–1592. https://doi.org/10.1016/j.nonrwa.2011.11.016

14. Q. Hou, L. Zhang, M. Liu, Mathematical analysis of a time-delayed model on brucellosis transmission with disease testing information, *Int. J. Biomath.*, **5** (2020), 2050039. https://doi.org/10.1142/S1793524520500394

15. Q. Hou, F. Zheng, Global dynamics of a general brucellosis model with discrete delay, *J. Appl. Anal. Comput.*, **6** (2016), 227–241. https://doi.org/10.11948/2016019

16. P. O. Lolika, S. Mushayabasa, Dynamics and stability analysis of a brucellosis model with two discrete delays, *Discrete Dyn. Nat. Soc.*, **2018** (2018), 6456107. https://doi.org/10.1155/2018/6456107

17. H. Wu, W. Chen, N. Wang, L. Zhang, H. Li, Z. Teng, A delayed stage-structure brucellosis model with interaction among seasonality, time-varying incubation and density-dependent growth, *Int. J. Biomath.*, **16** (2023), 2250114. https://doi.org/10.1142/S1793524522501145

18. S. A. Addis, A. Y. Desalegn, Comparative seroepidemiological study of brucellosis in sheep under smallholder farming and governmental breeding ranches of Central and North East Ethiopia, *J. Vet. Med.*, **2018** (2018), 7239156. https://doi.org/10.1155/2018/7239156

19. A. M. Almuzaini, An epidemiological study of brucellosis in different animal species from the Al-Qassim Region, Saudi Arabia, *Vaccines*, **11** (2023), 694. https://doi.org/10.3390/vaccines11030694

20. G. Sun, Z. Zhang, Global stability for a sheep brucellosis model with immigration, *Appl. Math. Comput.*, **246** (2014), 336–345. https://doi.org/10.1016/j.amc.2014.08.028

21. M. Li, G. Sun, Y. Wu, J. Zhang, Z. Jin, Transmission dynamics of a multi-group brucellosis model with mixed cross infection in public farm, *Appl. Math. Comput.*, **237** (2014), 582–594. https://doi.org/10.1016/j.amc.2014.03.094

22. S. Liu, S. Zhao, Z. Bai, Y. Lou, G. Sun, L. Li, Global dynamics of a degenerate reaction-diffusion model for Brucellosis transmission, *J. Differ. Equations*, **437** (2025), 113284. https://doi.org/10.1016/j.jde.2025.113284

23. P. van den Driessche, J. Watmough, Reproduction numbers and sub-threshold endemic equilibria for compartmental models of disease transmission, *Math. Biosci.*, **180** (2002), 29–48. https://doi.org/10.1016/S0025-5564(02)00108-6

24. P. van den Driessche, Reproduction numbers of infectious disease models, *Infect. Dis. Modell.*, **2** (2017), 288–303. https://doi.org/10.1016/j.idm.2017.06.002

25. X. Wang, X. Zhao, Target reproduction numbers for time-delayed population systems, *Math. Biosci.*, **381** (2025), 109384. https://doi.org/10.1016/j.mbs.2025.109384

26. Z. Shuai, J. A. P. Heesterbeek, P. van Den Driessche, Extending the type reproduction number to infectious disease control targeting contacts between types, *J. Math. Biol.*, **67** (2013), 1067–1082. https://doi.org/10.1007/s00285-015-0858-3

27. Z. Shuai, P. Van den Driessche, Modelling and control of cholera on networks with a common water source, *J. Biol. Dyn.*, **9** (2015), 90–103. https://doi.org/10.1080/17513758.2014.944226

28. Q. Liang, Precautions for use of brucellosis live vaccine (Strain S2)(in Chinese), *Chin. J. Vet. Med.*, **48** (2012), 90.